

GEO-HYDROLOGY OF GYPSUM KARST AREAS

876

THE GEOMORPHIC IMPLICATIONS OF THE GEO-HYDROLOGY  
OF  
GYPSUM KARST AREAS

By  
JULIAN JOHN DRAKE, B.A.

A Thesis  
Submitted to the School of Graduate Studies  
in Partial Fulfilment of the Requirements  
for the Degree  
Master of Science

McMaster University  
May 1970

MASTER OF SCIENCE (1970)  
(Geography)

McMASTER UNIVERSITY  
Hamilton, Ontario

TITLE: The Geomorphic Implications of the Geo-hydrology of  
Gypsum Karst Areas.

AUTHOR: Julian John Drake, B.A. (Oxford University)

SUPERVISOR: Dr. D. C. Ford

NUMBER OF PAGES: viii, 90

SCOPE AND CONTENTS: Gypsum karst areas in British Columbia and Wood Buffalo National Park, Alta.-N.W.T. are described. Investigation of the geo-hydrology of these areas, particularly specifically the saturation states of rising waters, is demonstrated to be a valuable tool in defining the major geomorphic processes acting. The combination of thermo-dynamic equilibrium studies of the gypsum and limestone processes serves to define zones within which the dominant controls of rock solution can be inferred.

The commonly accepted parameters of limestone solution equilibria (Picknett's curves) are examined and shown to be incorrect. Use of the parameters and indices presented in this thesis gives much better accordance with observed characteristics of karst waters

### ACKNOWLEDGEMENTS

Thanks are due to Dr. D. C. Ford for invaluable criticism at all stages in the preparation of this thesis; to Dr. T. M. L. Wigley for co-operation in the field (in the Canal Flats area); and to G. Pilkington and P. G. Fuller for untiring assistance in the field.

Financial assistance is gratefully acknowledged from the National and Historic Parks Branch, Department of Indian Affairs and Northern Development (for work in Wood Buffalo National Park) and the National Research Council of Canada.

Finally, the author is grateful for the willing co-operation of many members of the staff of the National and Historic Parks Branch, and in particular Mr. A. D. Adie, Superintendent, Wood Buffalo National Park; and of the staff of the Water Quality Division, Department of Energy, Mines and Resources, in Calgary and Fort Smith.

## T A B L E O F C O N T E N T S

### Chapter

One	INTRODUCTION	1
Two	ANALYTICAL METHODS AND TECHNIQUES	5
Three	WOOD BUFFALO NATIONAL PARK STUDY	
	I Wood Buffalo National Park	16
	II Geomorphological Implications of the Geo-hydrologic Networks	32
Four	THE CANAL FLATS AREA	
	I Description	48
	II Geomorphological Implications of the Hydro-chemical Study	62
Five	CONCLUSIONS	72
	APPENDIX A	81
	APPENDIX B	87
	BIBLIOGRAPHY	89

## LIST OF FIGURES

1.	A sample Water Quality Division water analysis report	13
2.	Wood Buffalo National Park	18
3.	Hydrologic zones within Wood Buffalo National Park	22
4.	The Salt River Area	28
5.	Karst features in the Salt River area	30
6.	Summary data for Slave River, 1968	35
7.	Summary data for Peace River, 1968	36
8.	Scattergram of the degree of saturation and discharge for Slave and Peace Rivers, 1968	37
9.	Hydrographs of the Slave, Peace and Athabasca Rivers, 1968	39
10.	Summary data for Benchmark Creek, 1968	43
11.	Regression of Discharge and SATGYP for Benchmark Creek, 1968	44
12.	The location of the canal flats area	49
13.	The Canal Flats area	50
14.	Dye test on east side of Coyote Creek	60
15.	Summary of hydrochemical data for Tufa Creek area and Phantom Sink Creek area	66
16.	Geologic cross-section of the Canal Flats area	68
17.	Modes of sinkhole development	70
18.	Degree of saturation of Peace River and Slave River, 1968	73
19.	Trombe graph for Peace River and Slave River, 1968	74
20.	Degree of saturation for samples in the Canal Flats area	75
21.	Trombe graph for samples in the Canal Flats area	76

List of Figures (cont'd)

- |    |  |    |
|----|--|----|
| 22 | Degree of saturation of Peace River and Salve River, 1968,<br>using Picknett's value for $V_s$ | 78 |
| 23 | Distribution of carbonate species for all values of pH   | 88 |

LIST OF TABLES

1.	States of the sulfate-calcium equilibrium	10
2.	Comparison of calculated and measured solubility values for calcium sulfate	11
3.	Correlation matrices between chemical parameters and discharge for Slave River and Peace River 1968	40
4.	Chemical parameters of hot springs in the Canal Flats area	58
5.	Summary data for Canal Flats area	63

LIST OF PLATES

1.	Small fissures above Salt River	20
2.	Muskeg-type vegetation developed to the west of the Peace Point - Fort Smith highway	21
3.	The dry bed of the Nyarling River	24
4.	The Salt River area	29
5.	The gypsum exposure on the Lussier River	52
6.	The gypsum exposure in sinkhole 1	53
7.	Aerial view of sinkhole 5	55
8.	Aerial view of sinkholes 7 and 8	56

## CHAPTER ONE

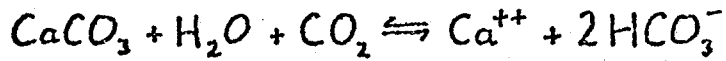
### INTRODUCTION

In all karst areas the dominant erosion process is solution. In no other domain is there such a clear-cut relationship between process and response, or is there such a degree of certainty that the process has not changed through time. If it is possible to assume that the dominant process is, and has been constant and to define this process, then it is possible to derive a quantitative process-response model. The success of this type of approach is dependent upon the description of the process involved. If this description is insufficiently detailed, then any model arising from it will of necessity contain a high degree of uncertainty.

No geomorphic process is independent in the sense that it is not in turn the response to some other, lower order, process. In the case of the karst solution process in limestone areas one of the major lower order processes is the availability of the reactant  $\text{CO}_2$  to the water. Estimates of  $\text{CO}_2$  partial pressure in the atmosphere vary significantly when quoted by various authorities working in similar areas. Measures of  $\text{CO}_2$  in soil air similarly show wide variation, although here the more important are those dependent upon the nature of the vegetation cover and the time of year. In the context of the karst solution process this problem has been discussed by Smith and Mead (1962) and a detailed consideration is presented by Pitty (1966 and 1968). Most of the common measuring

techniques for CO<sub>2</sub> involve the use of micro-probes which give a point reading; it is necessary to take many measurements to achieve a meaningful result for a given area. There are numerous other complexities postulated, but at present little is known of their quantitative effect. Picknett (1964) suggests that trace quantities of lead, scandium, copper, gold, manganese and other elements may depress limestone solubility in water by up to 50%. In many limestone systems there is also the possibility of other, related processes, such as the commonly quoted effect of soil derived acids and the natural or pollution-induced occurrence of many inorganic acids in, for example, rainwater near industrial areas. It is apparent that, although the limestone water system is seemingly well-defined, the problems of accurately describing many of the parameters are such that it is not possible at present to generate a quantitative process-response model.

Calcium carbonate is not the only rock forming compound which is dissolved to such an extent that solution by natural waters is the major erosion process. The gypsum/water system is in theory far simpler than that of limestone/water as it is not necessary for any reagents other than water and gypsum to enter the system. The process of carbonate solution may be represented as:



and that for gypsum as:



It can be seen that there are no exogenous factors to be considered in this simple model.

Much of the work published to date on karst processes has been

confined to limestone karst. There is little gypsum karst in Europe, and much of this is in East Germany. The Oklahoma-Texas gypsum has not until recently received much attention in a scientific and geomorphologic sense. In contrast, considerable work has been described in the U.S.S.R. on both gypsum and salt karsts, but, again the geomorphologic aspects have been largely subordinated to the geo-chemical and hydro-geologic aspects.

Several of the conclusions of these works may have geomorphic implications for karst areas in general, and for this reason it is thought that the study of a gypsum karst can be regarded as an initial step in an attempt to derive a process-response model for a general karst system.

A karst model of this type would be capable of yielding significant information on the groundwater regime of the area in terms of areal and temporal interactions. Zverev (1965) has shown that the simple  $Ca^{++}:SO_4^{--}$  ratio in a sulfate terrain is indicative of the hydrologic conditions, since the relative proportions of each ion depend on certain hydrologic and geologic parameters. Also, Back and Hanshaw (1965) state:

"Hydrochemical facies reflect the effects of chemical processes in the lithologic environment and the prevailing groundwater flow patterns."

If it proves possible to derive such a model for a karst system, an investigation of that system could be based on the measurement of simple variables such as the discharge and chemical composition of resurging waters, possibly eliminating the need for complex and costly water tracing projects.

This thesis describes two gypsum karst areas in Canada and illustrates that a knowledge of the hydro-chemistry of an area can be used in deriving empirical hydrologic relationships. In addition, certain accepted assumptions and techniques used in the study of limestone karst areas are examined.

## CHAPTER TWO

### ANALYTICAL METHODS AND TECHNIQUES

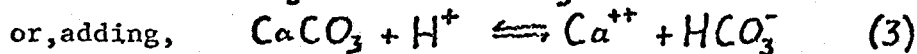
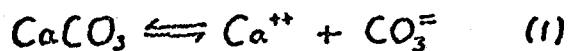
#### 1. The Theory of Saturation Indices

There have been several attempts in the past to describe the degree of saturation of ground water with respect to calcite by thermodynamic analysis. Larson and Buswell (1942) present a comprehensive review of the whole topic, while more recently Garrels and Christ (1965) give a detailed account of various types of carbonate equilibria. Back and Hanshaw (1965) state:

"... the most promising approach (towards an understanding of the limestone solution process)..... involves the application of concepts from chemical thermodynamics to hydrologic environments."

and Back, Cherry and Hanshaw (1966) illustrate this type of analysis in a study of the Florida karst ground water system. The following is based largely on the last mentioned study above.

Limestone solution can be expressed in many ways, but the most simplistic and pertinent is that expressed in terms of variables which can be measured in the field or in the laboratory:



The Law of Mass Action allows these reactions to be expressed in terms of thermodynamic processes:

$$\text{from (1), } K_s = (Ca^{++})(CO_3^{--}) \quad (4)$$

$$\text{from (2), } K_2 = \frac{(CO_3^{--})(H^+)}{(HCO_3^-)} \quad (5)$$

where quantities in brackets thus ( ) denote the thermodynamic concentration of the ion, and  $K_s$  and  $K_2$  are thermodynamic constants. (solid phase) is by definition unity. If chemical equilibrium and saturation exist, then  $K_s$  represents the solubility constant of calcite, and  $K_2$  the second dissociation constant of carbonic acid,  $H_2CO_3$ ; more generally they represent the appropriate ion activity product.

(4) and (5) may be combined to give

$$K_s = \frac{(Ca^{++})(HCO_3^-)K_2}{(H^+)} \quad (6)$$

Values of  $K_s$  and  $K_2$  are known, and  $(Ca^{++})$ ,  $(HCO_3^-)$  and  $(H^+)$  can be easily calculated from field measurements. This equation thus allows a simple calculation of the equilibrium state of the sample. If the calculated value for  $K_s$  (denoted by  $K_{sc}$ ) is less than the value of the solubility constant, then the sample is under-saturated with respect to calcite. The equation may be written more conveniently using a p - transformation where

$$pX = -\log_{10}(X)$$

this transformation is familiar in the case of hydrogen ion -  $(H^+)$  is invariably measured as pH. (6) thus becomes

$$pK_s = pCa^{++} + pHCO_3^- + pK_2 - pH \quad (7)$$

It is important to note, however, that this transformation reverses the sense of  $pK_s$  as compared to  $K_s$ . As  $K_s$  increases,  $pK_s$  decreases. Thus, if  $pK_{sc} < pK_s$  the sample is oversaturated. A convenient index of saturation is provided by

$$I = pK_s / pK_{sc} \tag{8}$$

I is known in this thesis as SATCAL.

A value for SATCAL of 1.0 indicates saturation, < 1.0 undersaturation and > 1.0 oversaturation. Back, Cherry and Hanshaw (1966) use the index

$$I' = (K_{sc} / K_s) \times 100\% \tag{9}$$

This, however, is unfortunate in that it suggests a linear relationship between I' and saturation, and indirectly between I' and (Ca<sup>++</sup>). A value of I' of 50% does not mean that there is one-half the amount of Ca<sup>++</sup> present that is necessary for saturation. SATCAL is used to create a cardinal scale with no implicit associations of direct proportionality to (Ca<sup>++</sup>). Thus far no assumptions have been made regarding (Ca<sup>++</sup>). This value, and those for other ions, represents thermodynamic concentration. If the total ionic strength of the sample, defined as

$$\Gamma = \frac{1}{2} \sum_i m_i z_i^2$$

where m<sub>i</sub> = molality of each ion  
z<sub>i</sub> = charge on each ion

is less than 0.001, the thermodynamic concentration can be assumed to be equal to the measured concentration without introducing a significant error. At values of Γ higher than this it is necessary to introduce the activity coefficient, γ<sub>i</sub>, defined such that

$$(X) = \gamma_x [X]$$

where [X] represents the molal concentration.

Values of γ can be calculated from the Debye-Huckel equation

$$\log_{10} \gamma_i = - \frac{A z_i^2 \Gamma^{1/2}}{1 + B a_i \Gamma^{1/2}}$$

where  $A, B$  are temperature dependant constants;  
 $\alpha_i$  represents the effective diameter of the ion  
 in solution;  $z_i, \Gamma$  are defined above.

Davies (1962) gives as a simplified version of the Debye-Huckel equation suitable for geo-chemical applications

$$-\log_{10} \gamma_i = A z_i^2 \left( \frac{\Gamma^{1/2}}{1 + \Gamma^{1/2}} \right) - 0.2 \Gamma$$

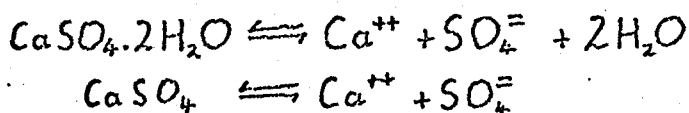
This is stated to be valid for  $\Gamma < 0.1$ , and has been used in computations in this thesis. Equation (7) thus becomes

$$pK_{sc} = p([Ca^{++}] \gamma_{Ca}) + p([HCO_3^-] \gamma_{HCO_3}) + pK_2 - pH \quad (10)$$

$\gamma_H$  is defined as unity.

$K_5$  and  $K_2$  are temperature dependant constants, and have been assumed to take direct values over 5°C intervals from 0°C to 25°C.

A similar procedure is followed for gypsum and anhydrite. In this case there is a considerable simplification as both minerals are readily soluble in water:



The ion activity product,  $K_G$ , is the same in both cases, as  $(H_2O)$  is, like (solid), defined as unity:

$$K_G = (Ca^{++})(SO_4^{=})$$

or,

$$K_G = [Ca^{++}] \gamma_{Ca} \cdot [SO_4^{=}] \gamma_{SO_4}$$

Saturation indexes can then be calculated as

$$SATGYP \equiv I = pK_G / pK_{Gc}$$

Values for  $pK_G$  are derived from Kramer (1969), and values for  $pK_5$  and  $pK_2$  are taken from Garrels and Christ (1965). Programs used in this thesis are given and described in Appendix A.

## 2. Other Analytical Methods

Zverev (1965) has suggested that the  $Ca^{++}:SO_4^{--}$  ratio might be capable of yielding information on the ground water regime. Table 1 is reproduced from Zverev, p. 119, and summarizes the effects producing the various states. The limits of the classes are not stated (i.e. the limits within which the ratio can be considered to be unity), but the general scheme is clear. The state  $Ca^{++} < SO_4^{--}$  may arise in a zone of sluggish water exchange in areas where the carbonate equilibrium is an important control of  $(Ca^{++})$ . The other two states arise in areas where the equilibrium is controlled by the gypsum solution process, but where this may be disturbed by other, mainly organic, processes such as bacterial action.

Metler and Ostroff (1967) describe an empirical method for calculating the value of  $K_c$  for solutions of high ionic strength and various excesses of one of the common ions. The errors introduced by assuming the Debye-Huckel equation in brines containing 58,460 mg/l NaCl is stated to be of the order of 200%. It is shown, however, that the errors introduced by this assumption in waters having an ionic strength of those in the two field areas of this study and where there is not great disparity between the  $Ca^{++}$  and  $SO_4^{--}$  concentrations are negligible. TABLE 2 is adapted from Metler and Ostroff, Table 1, and shows that the maximum likely error for the samples in this study (maximum values are: excess  $Ca^{++}=2.4$  meq/l;  $Na^+ = 509$  meq/l;  $Mg^{++} = 1.8$  meq/l) is of the order of 1%.

## 3. Analysis of Water Samples

Water sample data used in this thesis fall into two groups - those

Table 1. States of the sulfate-calcium equilibrium.

From Zverev (1965), p119.

Equation determining the sulfate-calcium equilibrium	$\gamma_{CaSO_4} [Ca^{++}] [SO_4^{--}] = K_{CaSO_4}$		
Quantities influencing the equilibrium as a whole	Temperature and pressure for $K_{CaSO_4}$ and $\gamma_{CaSO_4}$ Total ionic strength of solution, $\Gamma$ , for $\gamma_{CaSO_4}$		
Kind of equilibrium	$Ca^{++} > SO_4^{--}$	$Ca^{++} \sim SO_4^{--}$	$Ca^{++} < SO_4^{--}$
Type of $Ca^{++}$ and $SO_4^{--}$ dynamics in solution	Removal of $SO_4^{--}$ from solution and entry of $Ca^{++}$ into solution	Simultaneous entry of $Ca^{++}$ and $SO_4^{--}$ into solution	Removal of $Ca^{++}$ from solution and entry of $SO_4^{--}$ into solution
Hydrogeologic condition governing kind of equilibrium	Sluggish water exchange in hydrogeologically closed structures	Intense water exchange in areas of gypsum and anhydrite	Sluggish water exchange in hydrogeologically open structures
Processes determining the kind of equilibrium	Microbiologic activity Reduction of organic matter. Cation exchange	Solution of gypsum and anhydrite	Oxidation of sulfides Precipitation of gypsum High $CO_3^{--}$ content Cation exchange
Type of oxidising - reducing environment and solution alkalinity	Acid reducing environment	Neutral oxidising environment	Neutral and alkaline oxidising-reducing environment

Mg <sup>++</sup> (meq/l)	Excess Ca <sup>++</sup> (meq/l)	Calculated solubility if Na <sup>+</sup> (meq/l) =		Measured solubility if Na <sup>+</sup> (meq/l) =	
		0	1000	0	1000
0	0	2.09	6.26	2.01	6.05
0	250	1.17	3.51	0.80	2.61
400	0	5.64	16.90	5.68	7.26
400	250	3.16	9.47	2.19	3.02

Table 2. Comparison of calculated and measured solubility values  
(in gm/l) for calcium sulfate at 28°C.

From Metler and Ostroff (1967), Table 1

samples collected and analysed by the Water Quality Division, Inland Waters Branch, Department of Energy, Mines and Resources, and those analysed in the field.

a) Water Quality Division data

This data is part of the routine sampling network established by the Calgary office of the Division, and is complete for a wide range of elements, ions and physical properties. A sample sheet is reproduced in FIGURE 1. The samples are collected in glass containers and a field measurement of temperature taken. They are then analysed in the Calgary laboratory within 2 - 3 days. The analytical methods used are accurate to within 2 parts per million (ppm) (Lesick, pers. comm.), except for pH, where the error is  $\pm 0.05$  unit. A potentially more serious source of error is the deterioration of samples between collection and analysis. Previous experience at McMaster suggests that the calcium ion may be absorbed onto certain types of plastic containers, and that over periods of greater than a few days precipitation of calcium carbonate may occur. In addition it has been demonstrated that the carbon dioxide content of a sample changes rapidly after collection (particularly if it is stored in a polyethylene container, which is porous to the gas) with a consequent change in pH. Water Quality Division practice of rapid analysis and the use of glass containers eliminates most of these problems, and tests conducted by Lesick suggest that the change in pH is no more than 0.2 units, part of which error is attributable to the difference in temperatures of the sample when collected and when analysed.

The reliability of the measurements of the most common ions is indicated by the ion balance error, which is generally less than



$\pm 3\%$ .<sup>1</sup> This value is a combination of individual measurement errors, and errors introduced by the non-measurement of any other ions which may be present. It can be seen from Figure 1 that the important ions are  $\text{Ca}^{++}$ ,  $\text{Mg}^{++}$ ,  $\text{Na}^+$ ,  $\text{HCO}_3^-$ ,  $\text{SO}_4^{--}$  and  $\text{Cl}^-$ . A calculation of the ion-balance error using only these ions results in a change in the error of only 0.7% (from 2.8% to 2.1%). The dangers inherent in the interpretation of such error measurements are well illustrated by this instance - ignoring certain ions leads to an apparent reduction in the overall error - but as a general rule an ion balance within  $\pm 5\%$  indicates that no serious measurement errors have been made, and that no significant deterioration of the sample has occurred.

b) Field analysis of water samples

On the basis of the above, field analyses were limited to temperature, pH,  $\text{Ca}^{++}$ ,  $\text{Mg}^{++}$ ,  $\text{Cl}^-$  and  $\text{HCO}_3^-$ , with subsequent laboratory analysis for  $\text{SO}_4^{--}$ . Two systems of field measurements for  $\text{Ca}^{++}$ ,  $\text{Mg}^{++}$  and  $\text{HCO}_3^-$  were employed, both being a set of volumetric titrations. The first consisted of the standard Schwarzenbach EDTA titrations for  $\text{Ca}^{++}$  and  $\text{Mg}^{++}$  using British Drug Houses standard reagents (for a full description and bibliography of this method see Douglas 1968) and a potentiometric titration with HCl for  $\text{HCO}_3^-$  (see Appendix B for details of procedure). The second system was a self-contained commercial analysis

---

<sup>1</sup>The ion balance error is calculated as

$$E = \frac{\sum \text{cation} - \sum \text{anion}}{\sum \text{cation} + \sum \text{anion}} \times 100 \%$$

where  $\sum \text{cation}$  is the sum of all cations expressed in equivalents/liter, and  $\sum \text{anion}$  the similar sum for all anions.

kit for  $\text{Ca}^{++}$ ,  $\text{Mg}^{++}$  and  $\text{HCO}_3^-$  manufactured by the Hach Chemical Company of Iowa. This system is by far the more rapid and portable, but the accuracy is only of the order of  $\pm 8\text{ppm.}$ , comparing unfavorably with the  $\pm 2\text{ppm.}$  obtainable by the Schwarzenbach method.

For all samples temperature was measured with a mercury in glass thermometer graduated in  $0.1^\circ\text{F}$  or  $^\circ\text{C}$ , and pH by either a colorimetric meter or by a portable Metrohm meter calibrated between pH7 and pH10.4. The accuracy of the colorimeter is estimated to be  $\pm 0.5$  unit, and of the Metrohm meter  $\pm 0.05$  unit.

Laboratory analysis of all samples for  $\text{SO}_4^{=}$  followed the method described by Rainwater and Thatcher (1960), which is the standard method used by the U.S. Geologic Survey. The accuracy of the method is  $\pm 1\text{ppm.}$  in the range 10-999 ppm. Chloride was measured in the field by a volumetric titration kit manufactured by the Hach Co., but the accuracy was so low ( $\pm 25\text{ppm.}$ ) to preclude the use of the results. A more accurate ( $\pm 1\%$ ) estimate was obtained in the laboratory by the use of an Orion specific electrode system.

No field method exists for the measurement of  $\text{Na}^+$ , and laboratory determinations are complex (usually spectrophotometric). Since it is necessary to know the total ionic strength to calculate activity coefficients it is assumed for the purposes of this thesis that all  $\text{Cl}^-$  present is associated solely and completely with  $\text{Na}^+$ , and thus that  $\text{Cl}^-$  is a measure of  $\text{Na}^+$ . The problem is only significant in the case of very few samples, since in one of the study areas (Canal Flats) the total ionic strength is sufficiently low to make activity values almost unity, and most samples in the other study area (Wood Buffalo National Park) have been analysed by the Water Quality Division.

## CHAPTER THREE

### I. WOOD BUFFALO NATIONAL PARK

#### 1. Introduction

Two field areas were chosen to investigate the geomorphological significance of the type of analysis described above. Gypsum deposits in Canada are few, and are widely separated. The two areas concerned here represent very different types of deposit. One, in Wood Buffalo National Park, Alta.-N.W.T., is extensive, of low relief and relatively simple geology; the other, near Canal Flats, B.C. is much smaller, has considerable local relief and is in an area of complex structural geology. In detail, little is known of the geology or geomorphology of either area, especially in the case of Wood Buffalo National Park where no geomorphological work per se has been undertaken. For this reason much of the following description is broad and qualitative in nature. Considerable work in all branches of the discipline would be necessary to substantiate or disprove many of the tentative conclusions, but most of these do not have any immediate bearing on the content of the present thesis.

#### 2. Wood Buffalo National Park

Wood Buffalo National Park is the largest National Park in Canada, occupying some 17,000 sq. miles and lying across the N.W.T.-Alberta

boundary. The gypsum area comprises some 60% of this area, and is bounded to the south by the Peace River, to the west by the Caribou Hills and to the north and east by an escarpment 50 feet to 200 feet high which rises above the Great Slave Lake and Slave River lowlands (see Figure 2). The escarpment lies below the 800' contour shown and diminishes in height to the south. It probably marks a previous shore of the Great Slave Lake. No geological maps exist. Camsell (1917) is the only published source and although it is understood that major oil companies have compiled more detailed information, this is not at present available. There are only four exposures of the principal formation. These are all natural exposures along the Peace, Slave and Salt rivers. The Peace River section is described by Camsell as follows:

"The lowest bed is of gypsum, the thickness of which is variable but has an exposed maximum of 50 feet. The next overlying bed is a fractured and broken dolomite from 10 to 30 feet thick, above which is an argillaceous, sometimes sandy limestone containing fossils. Overlying all is the drift from 5 to 20 feet in thickness. The beds undulate in both sharp and gentle folds and in one place are bent into a sharp anticline with dips on either limb of 60 degrees. The strike of the folds is not constant but varies widely".

The only other section to expose gypsum is that formed by the escarpment above the Salt River. Only in the case of the atypical anticline are there any measurements of dip or strike.

The structure of the Park is apparently simple. The bedding nowhere shows dips of more than 5° but there are numerous severe local disruptions. The most spectacular comprises a tightly folded anticline which appears to the south of the Peace River, 1 mile upstream of Peace Pt. The dip on both limbs is of the order of 60°. Similar, but lesser

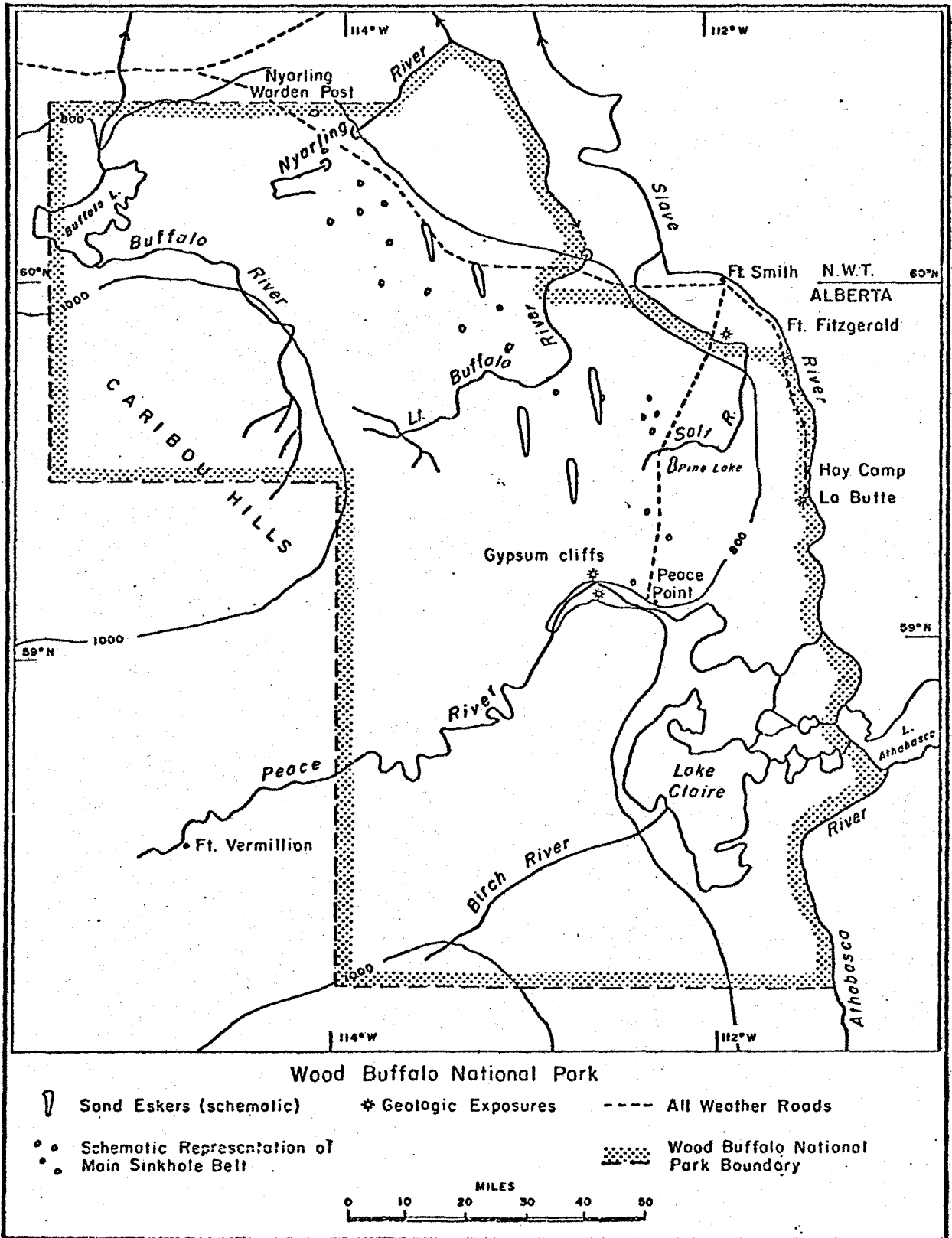


Figure 2. Wood Buffalo National Park.

features are found in the area of the Salt River bridge. Here the terrain is composed of a number of large fissures and ridges. The ridges have an anticlinal structure and there is evidence of disruption at the ridge fissure junctions. Similar, but smaller fissures are shown in Plate 1. Camsell (p. 137) attributes such features to the 33% volume expansion consequent on the conversion of anhydrite to gypsum. Nodules of anhydrite appear in the gypsum bed in most localities and are generally surrounded by a crust of gypsum.

The drift mentioned by Camsell overlies the whole of the Park, and is of varying composition although it is probably all Wisconsin Glacial drift. To the west of the Ft. Smith - Peace Point highway it is generally heavy and clayey, supporting a muskeg type vegetation (Plate 2). To the east of the highway, and in a belt immediately north of the Peace River it appears to be sandy, with little or no muskeg development. It is possible that the distribution of muskeg is controlled largely by the hydrology of the area. There are three hydrologic zones (Figure 3) within the Park above the escarpment. The Caribou Hills form the inner zone, supporting a well developed surface drainage network with a gradient of the order of 2000' over 30 miles. At the foot of this zone the surface network degenerates on the extremely low gradient plateau (the gradient is 200' over 30 miles) and gives rise to a waterlogged surface supporting the development of muskeg. Although the subsurface rocks are porous, the groundwater gradient is so small that there is little groundwater movement from this zone. The third zone is that immediately above the escarpment. The surface gradient is similar to that of the second zone (100' over 15 miles), but the presence of the escarpment allows

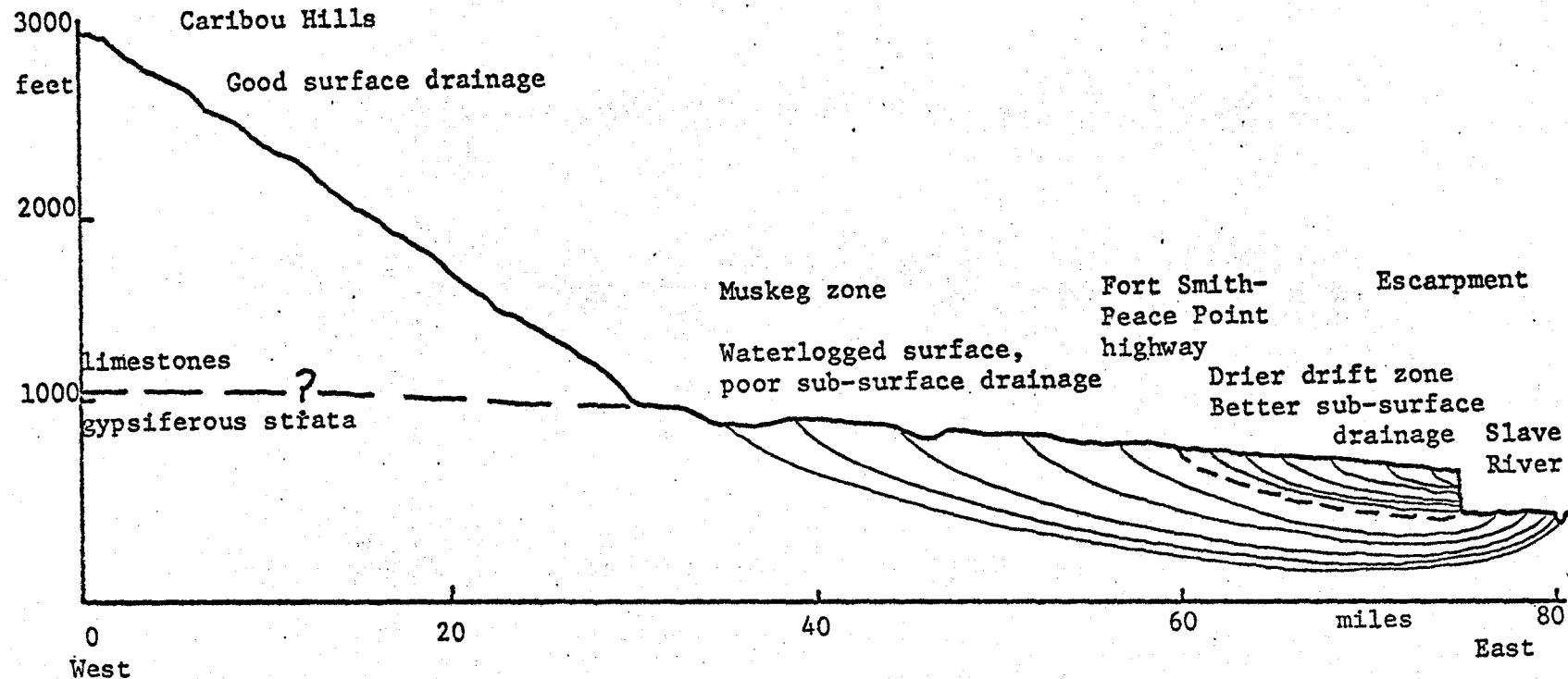


Plate 1. Small fissures above Salt River, west of the Peace Point - Fort Smith highway.



Plate 2. Muskeg type vegetation developed to the west of the Peace Point - Fort Smith highway.

Figure 3. Hydrologic zones within Wood Buffalo National Park.



the more rapid movement of groundwater and hence the surface drift remains drier than in the central zone.

A hydrologic explanation for the distribution of muskeg rather than one based on differences in drift texture is supported by the presence of sandy eskers in the muskeg areas, suggesting that there are no radical differences in drift composition within the Park.

### 3. Drainage and karst features

The drainage of Wood Buffalo National Park is very ill-defined. As noted above, the surface drainage net developed on the Caribou Hills degenerates on the plateau. With the exception of the Buffalo River, the Little Buffalo River and the upper reaches of Salt River there are no integrated surface flows above or across the scarp. This pattern is to be expected in an area of very low relief (a maximum of 150 feet over a minimum linear distance of 50 miles) and thick drift cover. The internal relief caused by the pattern of drift dumping is in all areas far more significant than the overall relief gradient. Below the escarpment to the east and north of the plateau there are a number of small streams flowing parallel to it and eventually draining to the Salt, Little Buffalo or Buffalo Rivers.

The lack of a surface drainage network and the presence of soluble and porous rocks suggests that groundwater flow is the significant factor in the hydrology of the area. There is only one instance of an underground network with definite sink and rising points. The Nyarling River is dry for some eight miles of its course (Plate 3) and it is understood (Novacowski, 1969) that it sinks into a large sinkhole and rises from a number of ill-defined points in the dry river bed. These

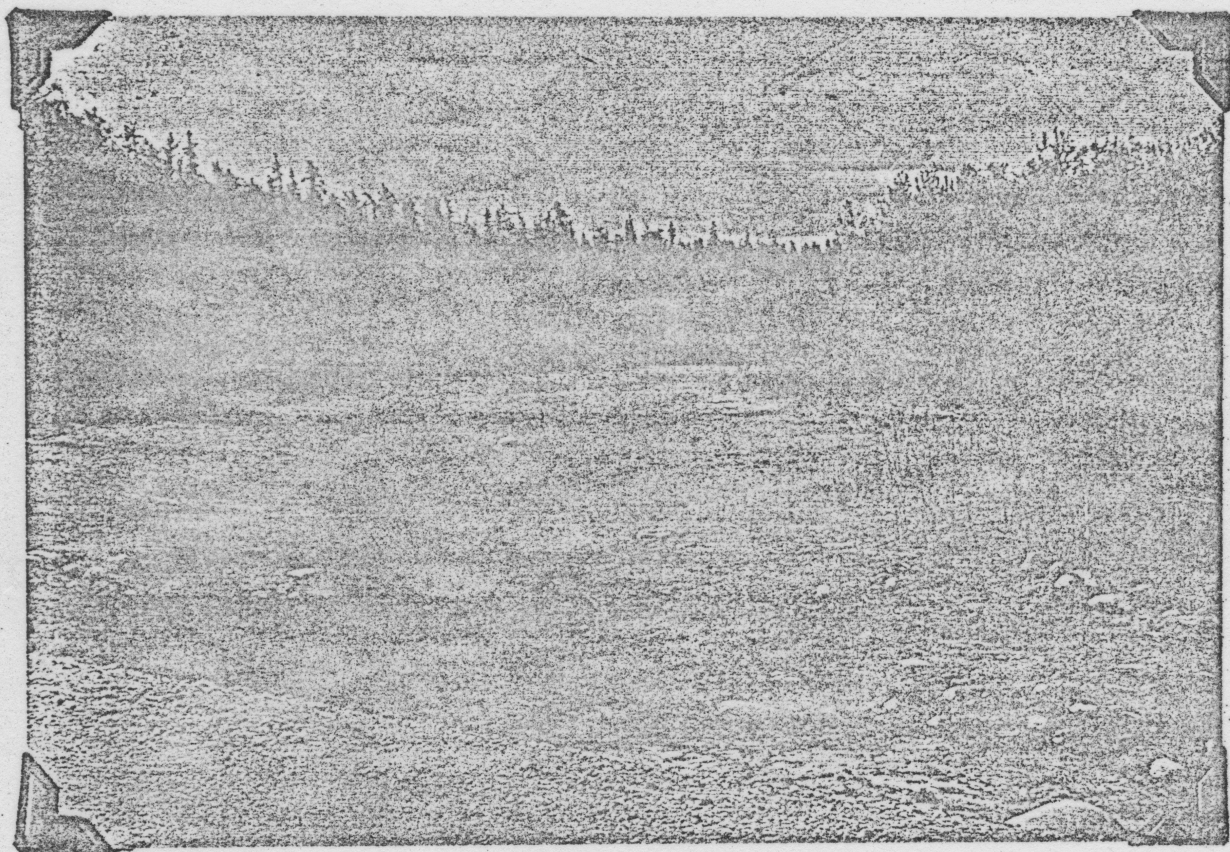


Plate 3. The dry bed of the Nyarling River, by the Hay River - Fort Smith highway.

areas were not accessible in May 1969, so no investigation of this phenomenon was possible. The whole Nyarling River area has been described as "a land of underground streams" (Soper, 1941), but it is doubted that this refers to an integrated underground system in the classical karstic sense. It is also understood from Novacowski that in periods of extremely low flow the Little Buffalo River sinks below the waterfall at the escarpment and rises some 1000 yards downstream.

Much of the drainage on the plateau is in the form of an ill defined groundwater movement. Brandon (1965) describes a potentiometric model of the groundwater flow along the line between Buffalo Lake and the Slave River in which the fixed points are defined by the dissolved solids concentration in Buffalo Lake, the Little Buffalo River and Slave River. The model demonstrates the probable existence of such a groundwater network, and represents the only form of description available, as in the absence of definite, accessible sink and rising points it is not possible to define a flow pattern by tracer methods such as that of Brown, Wigley and Ford (1969).

#### 4. Sinkholes

Sinkholes occur in the Park in a broad crescentic belt sweeping from the Nyarling River area in the north to Peace Point in the south (Figure 2). It is impossible to give an accurate estimate of their number, but it is thought to be of the order  $10^3$ . There are two broad categories of sinkhole:

a) those which are fairly large (diameters greater than 50 feet). These are relatively infrequent, water filled (with one exception) and occur within the muskeg area. The largest, Pine Lake, has been mapped

and is an agglomeration of three smaller features, the deepest of which is 70' deep. Slope angles in this instance are less than 40°.

b) those which are much smaller (having a typical diameter of less than 20 feet, and which are dry. These occur in the drier areas of the plateau and many give the impression of having suffered recent collapse, as their sides show considerable shear development. The sinkholes are widely dispersed within the belt, and appear to be clustered, although it is not possible to test this since only the large instances appear on air photographs, and the size of the belt prevented field investigation in the limited time available.

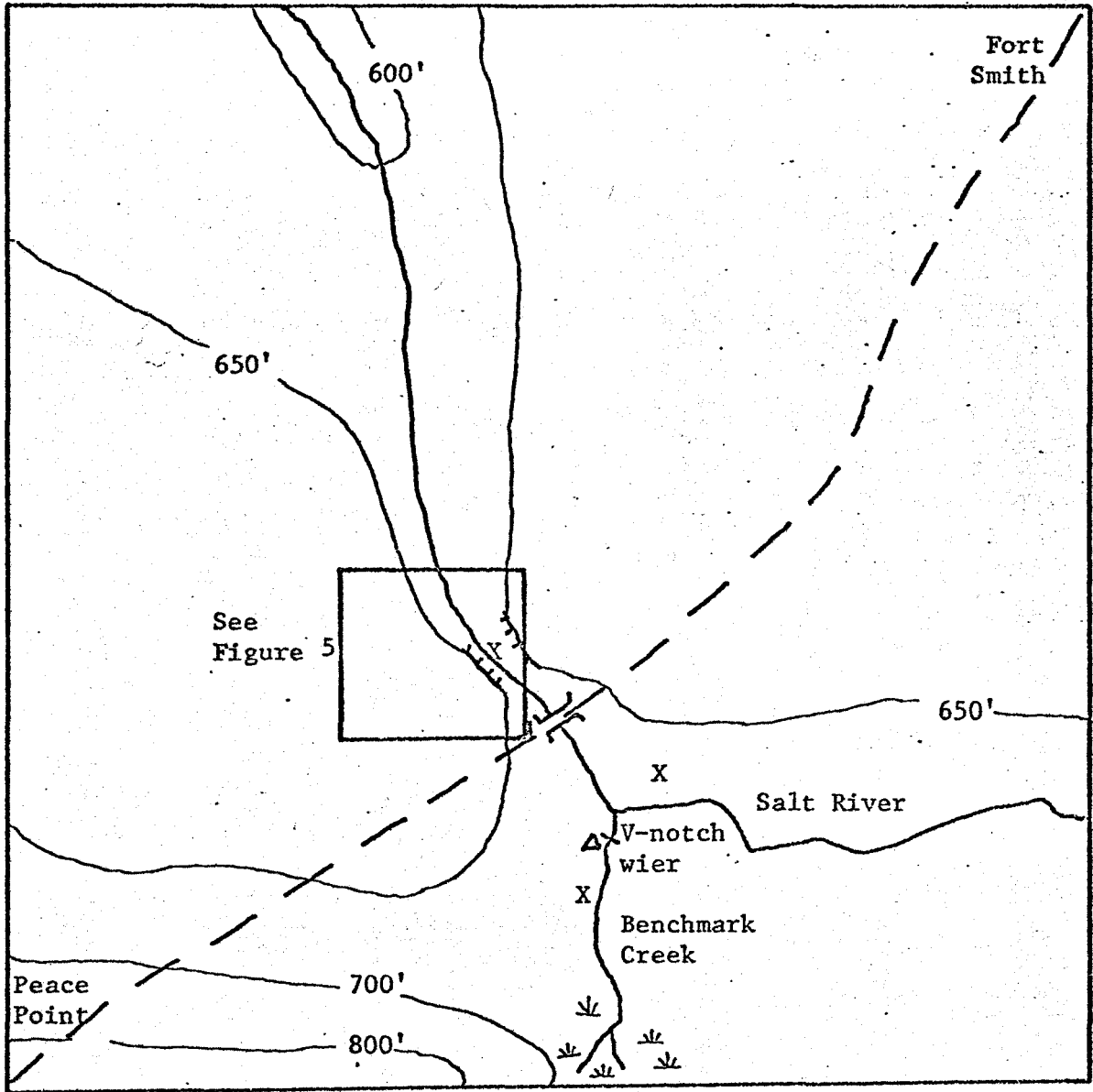
The one exception mentioned under (a) above is the sinkhole at the Nyarling Warden Station. This is the largest example in the Park, and is the only case which exposes rock sides. It is conical in shape, 180' deep by 300' across with 20' - 30' vertical cliffs at the top. Water occupies the lower 15 feet. In the absence of any depth sampling equipment it proved impossible to determine if sinkhole water was part of the surface runoff regime or if these features intersect the main groundwater body. Lack of any geologic information prevents the testing of any hypothesis of sinkhole location or development.

##### 5. Field programme

The present field study of the Wood Buffalo Park area was designed to test the hypothesis that groundwater regimes may be described by chemical data of endogenic waters, that the hydrology network of such areas may in part be deduced from this and that it is meaningful to attempt an analysis on the basis of the model outlined above (Ch. II). During the spring much of the park is inaccessible as summer roads are

waterlogged and the winter trails have thawed, thus severely limiting the possible range of sampling points. In addition, the short time available for this study necessitated the choice of sites to those for which data could be compared to long term data collected by the Water Survey of Canada. These logistical problems made it necessary to choose a limited area easily accessible during May. The area around Salt River was chosen as being the most developed karst area found in the Park.

Figure 4 illustrates the area. It is the only site visited in which conduits can be seen leading from the sinkholes and fissures, although Novacowski states that some are found in the Upper Nyarling area. Exposure of the bedrock in caves in the Salt River area allow the confirmation of the anticlinal structure of the ridges and the sampling of the groundwater network. Benchmark Creek is a Water Survey gauging and sampling site, but records only exist for 1968. The creek is extremely saline. It appears to rise from many indistinct points in a series of salt flats. Salt River has excavated a channel up to 60' deep through the fissure and ridge system (Plate 4). It is less saline than Benchmark Creek, but is still far from being potable. A number of spot samples were taken at the locations indicated on Figure 5. The major caves were mapped and are shown in Figure 5. At the time of the field study some were partially coated with a particularly delicate type of ice formation comprising masses of hollow hexagonal prisms  $\frac{1}{4}$ " across and  $\frac{1}{2}$ " long. In the caves exhibiting these crystals the final sump was frozen. The ice formations appeared to be melting from the top of the chamber down, and were absent from caves in which the final sump



0 1 2 3 miles

X Sampling sites

Cliff

Δ D.O.T. meteorological site

Figure 4. The Salt River area, Wood Buffalo National Park.

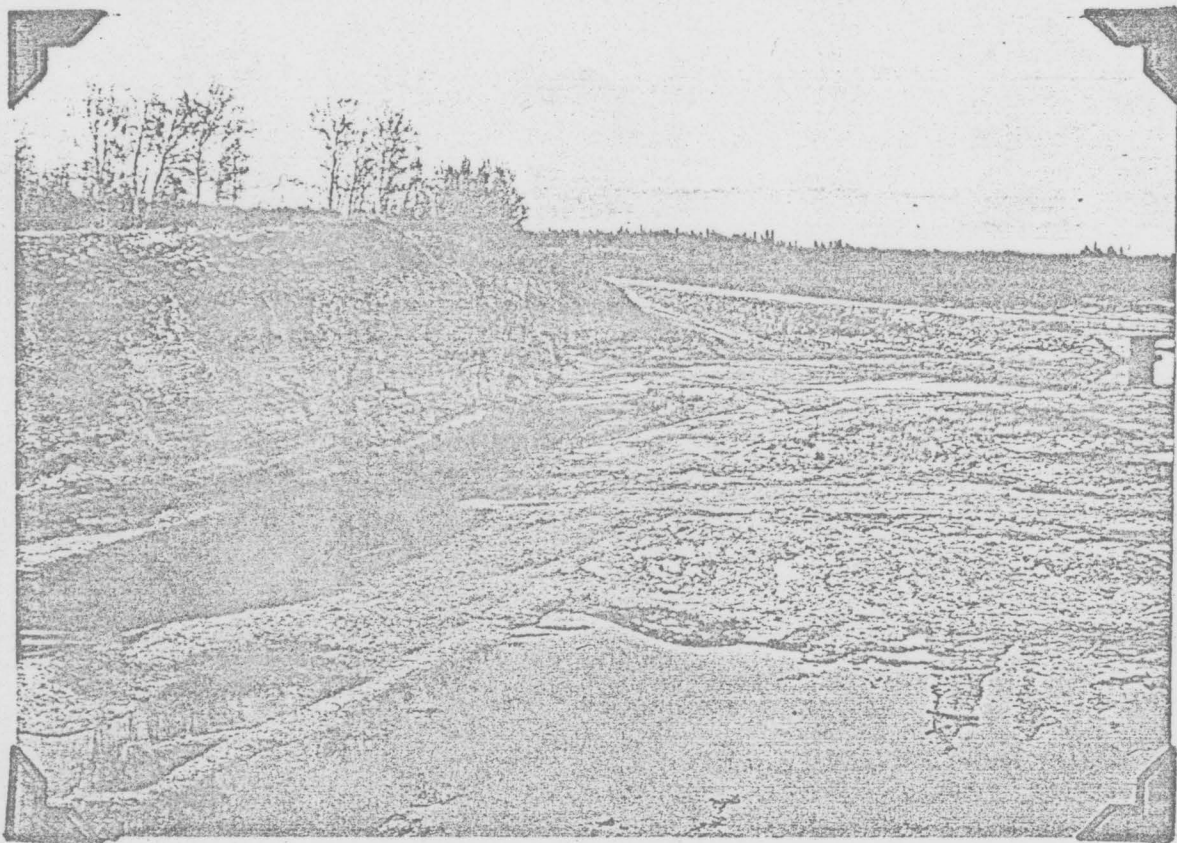


Plate 4. The Salt River area.

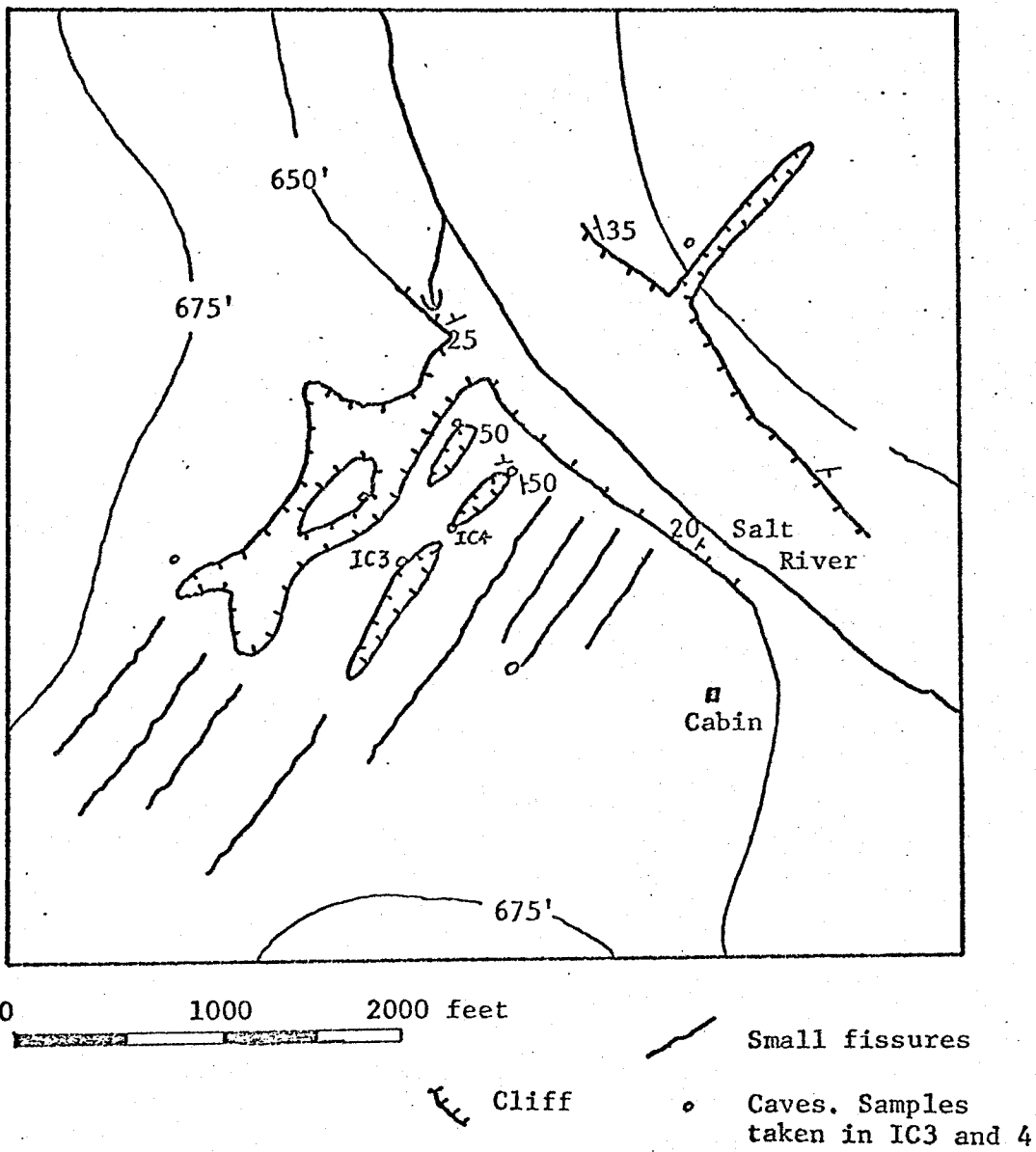


Figure 5. Karst features in the Salt River area.

was not frozen. There was no other evidence of frozen groundwater in the study area. It is unlikely that the groundwater network was seriously affected by ice formation, but it is possible that local interferences were present.

In addition to the Salt River area samples were taken of the water in the type (a) sinkholes. A depth-sampler was not available for this period, so no meaningful system of sampling groundwater flow in such locations was possible.

## II. GEOMORPHOLOGICAL IMPLICATIONS OF THE GEO-HYDROLOGIC NETWORKS

Water quality data for this field area fall into two groups: that for the Peace and Slave Rivers, and that for the Salt River area. The analysis is similarly in two stages - a broad investigation of the value of the saturation indices compared with untransformed concentration data and a detailed consideration of the use to which chemical data can be put in a small area.

### 1. An evaluation of the saturation indices as hydrologic indicators

It has been accepted that, in theory, the relationship between chemical parameters and discharge can lead to the deduction of certain facts about the hydrologic network concerned, although no predictive models have been formulated. Pinder and Jones (1969) describe a method of estimating the proportion of groundwater in the total flow of a surface stream and conclude that:

"The groundwater component of stream discharge estimated from the chemical characteristics of total runoff indicates that ..... groundwater forms a large part of peak flow".

Pinder and Jones assumed that the chemical parameters of groundwater flow do not vary with discharge and, thus, the ratio between chemical parameters of the stream at base flow (assumed to be 100% groundwater) and at other flows gives an indication of the ratio of groundwater flow to surface runoff. The existence of a relationship between discharge and  $\text{Ca}^{++}$  concentration from karst risings has been noted by many workers, and is of

interest from the point of view of cave formation, since it is desirable to determine which combinations (if any) of concentration and discharge are quantitatively the most important. A consideration of one chemical parameter together with discharge is of limited value since, although this may be used to obtain a value for the amount of limestone removed under given conditions, it cannot yield any information as to potential erosion. Ashton (1966) used pH,  $\text{Ca}^{++}$  concentration and flow measurements from the outlet of an underground system resulting from a flood pulse (either natural or artificial) applied to the sink point(s) to hypothesize the extent of looping, the vadose:phreatic length ratio and the degree of constriction within caves. He describes a test of this method in the Kolmos system, using data compiled by Jakucs (1959), which unfortunately is not conclusive as no independent description of the system is available. There appears to have been only one further application of Ashton's scheme, that of Atkinson and Drew (1967) in the Mendips, but here results are unsatisfactory, possibly due to the logistic difficulties involved in sampling several parameters over a number of hours following a sudden rainfall sufficient to induce the required pulse.

It appears possible that sophisticated statistical techniques (particularly spectral analysis) can resolve the problem of reliance on a single, natural pulse. In this case, however, long-term data for the output parameters are necessary and the technique itself loses the essential simplicity of the original. Ford (1966) has used a Trombe graph (plotting pH against  $\text{Ca}^{++}$ ) to illustrate the behaviour of cave waters in the Mendips as they flow through the system. It is, however difficult to relate this to discharge in a graphical display.

The index of saturation with respect to calcite, SATCAL, is a single variable combining pH, and  $\text{Ca}^{++}$  and  $\text{HCO}_3^-$  concentrations, and can thus be used to describe the behaviour of a series of samples consequent upon changes in other factors.

Figures 6 and 7 illustrate the variation of  $\text{Ca}^{++}$ ,  $\text{HCO}_3^-$ , pH, saturation with respect to calcite and discharge in 1968 for the Slave and Peace Rivers. They also indicate the relationships between the saturation index and its constituent variables. It can be seen that the index is most sensitive to pH, as in July the index and pH rise, whilst  $\text{Ca}^{++}$  and  $\text{HCO}_3^-$  decline. The reverse situation is apparent for the Slave River in June. This type of dependence is to be expected since it is the transformed p-variables which are used in calculating the saturation indices. It can be seen from Figure 8 that there is no simple relationship between flow and saturation. Also, from Figures 6 and 7 there is a far greater variation in flow than in any of the chemical variables parameters for which peak values are no more than 150% of the minimum. Comparison of discharge and ionic concentrations from Figures 6 and 7 is in many ways unsatisfactory as the chemical data is discontinuous, whilst the flow data can be regarded as continuous as it is compiled from daily records.

The Slave River at Ft. Fitzgerald represents the combined flows of Peace River and the Athabasca River, together with the local drainage of Lake Claire and Lake Athabasca and a number of tributaries to the east. It can be seen from the hydrographs of the three major rivers that all rivers have a peak flow in late June, and that minor peaks in the Peace

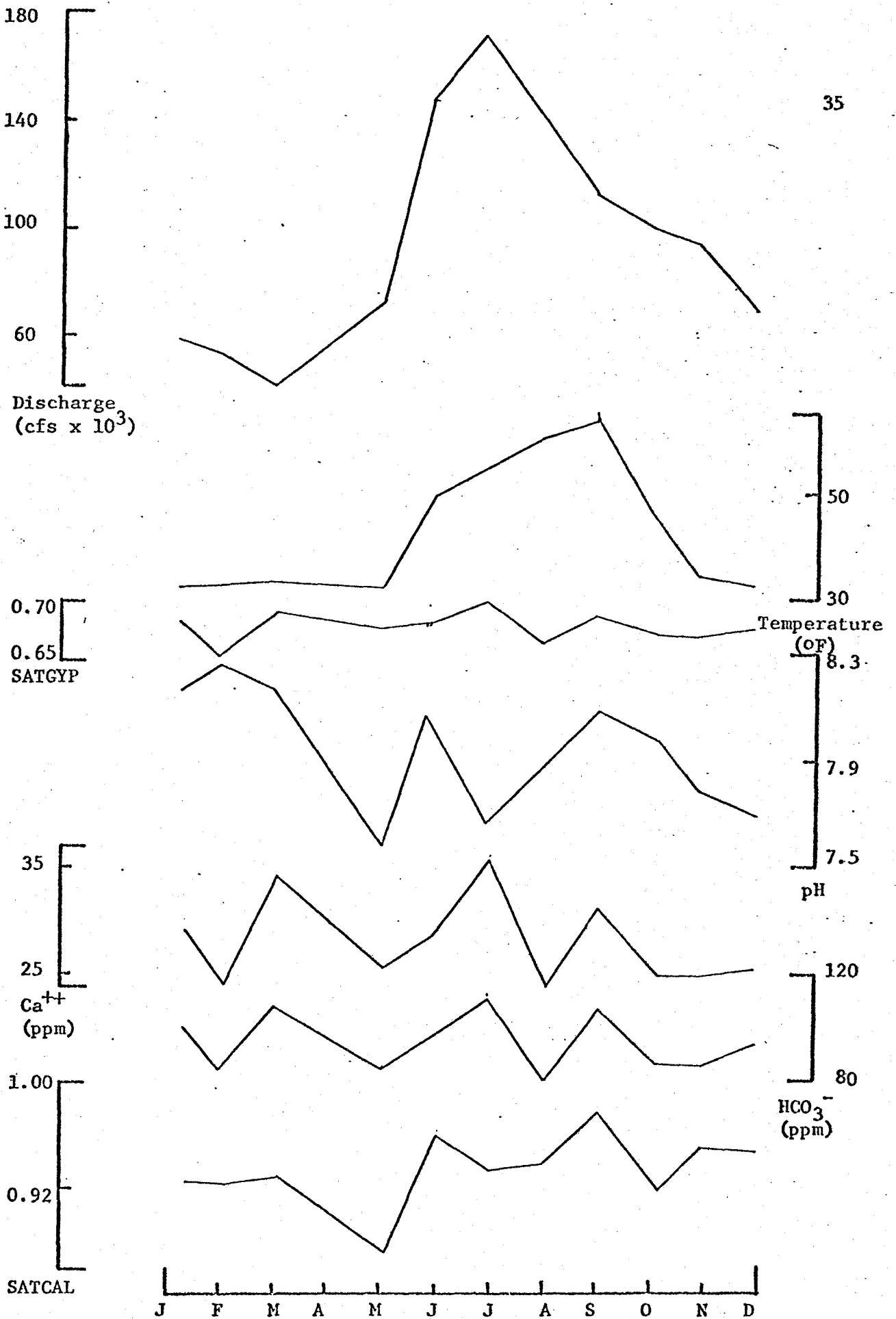


Figure 6. Summary data for Slave River, 1968.

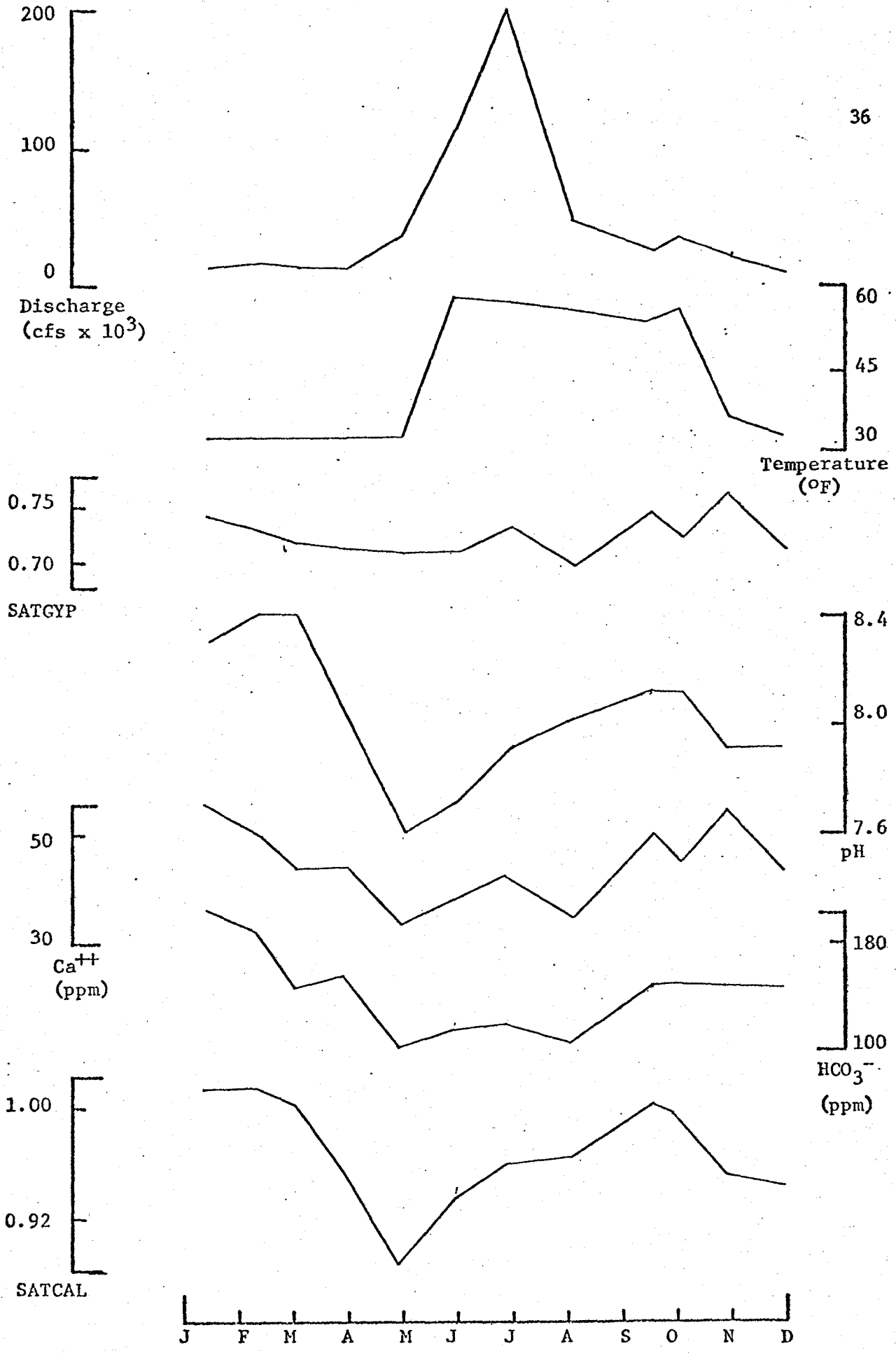


Figure 7. Summary data for Peace River, 1968.

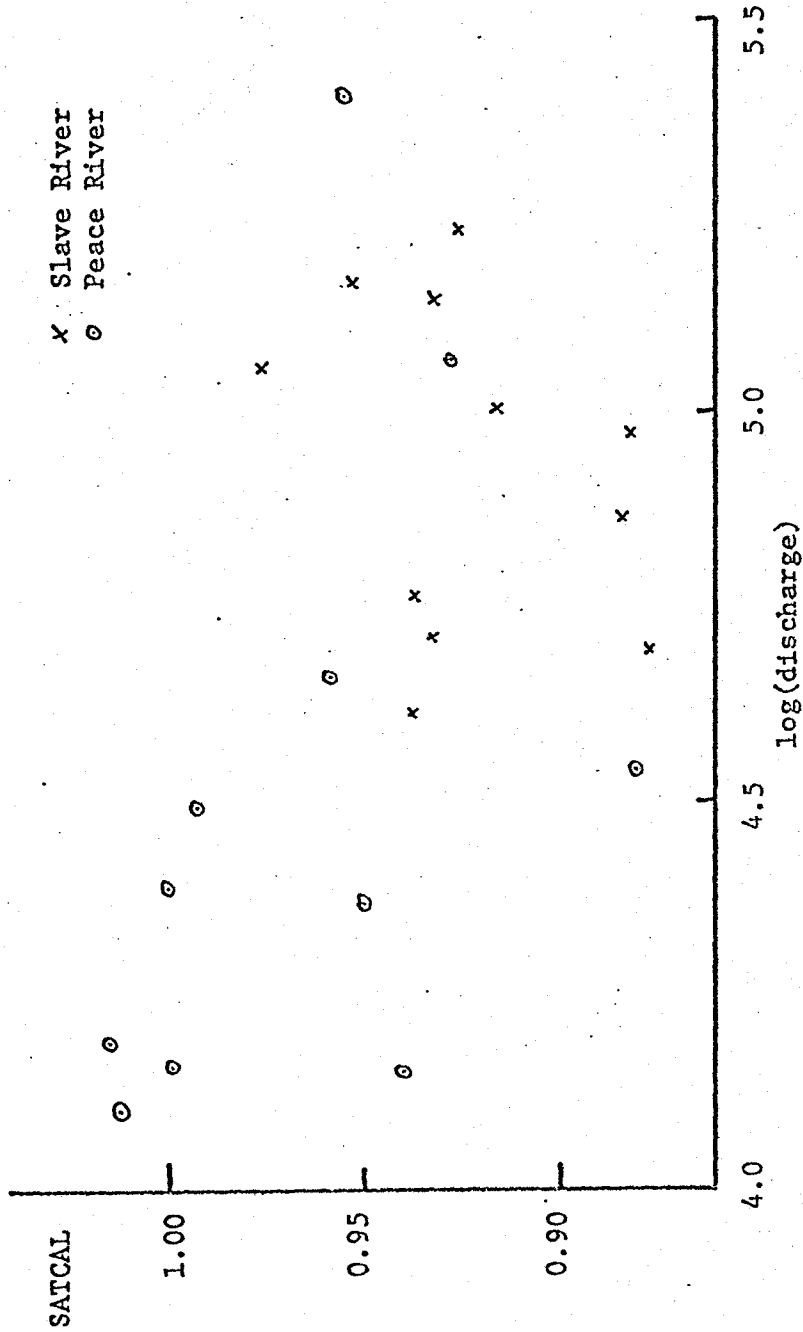


Figure 8: Graph of degree of saturation against discharge on a logarithmic scale for Peace and Slave Rivers, 1968.

and Athabasca rivers in mid-May, early June and mid-July serve to broaden the discharge curve of the Slave River (Figure 9). Since it is known that groundwater chemistry in karst areas is a function of discharge the Pinder and Jones method is not applicable to this situation. Empirical information can be extracted from a comparison of the flow and concentration curves for the rivers involved, but the lack of a known relationship prohibits any quantitative estimates.

The fall in SATCAL of the Slave River in March and April is consequent upon the fall in SATCAL for the Peace River. In both rivers the flow begins to rise in April. The rise in SATCAL is interpreted as a fall in groundwater flow consequent on the exhaustion of unfrozen reserves in March and a rise in direct runoff from snowmelt in April. Thereafter the proportion of groundwater rises, as evidenced by rising SATCAL in May for the Slave River and from May through September for the Peace River. The Slave River shows a temporary decline of SATCAL during June, and does not regain the late May value until mid-August. This is taken to reflect the input of an increasing flow from the Athabasca River during June and July.

TABLE 3 shows the simple correlation matrices between selected variables for the Slave and Peace Rivers in 1968. The correlations significant at the 5% level are:

<u>Peace River</u>		<u>Slave River</u>	
between Ca and pH		Ca and SO <sub>4</sub>	
Ca	SATCAL	pH and SATCAL	
Ca	SO <sub>4</sub>		
pH	SATCAL		

Since there is a theoretical relationship between Ca, pH and

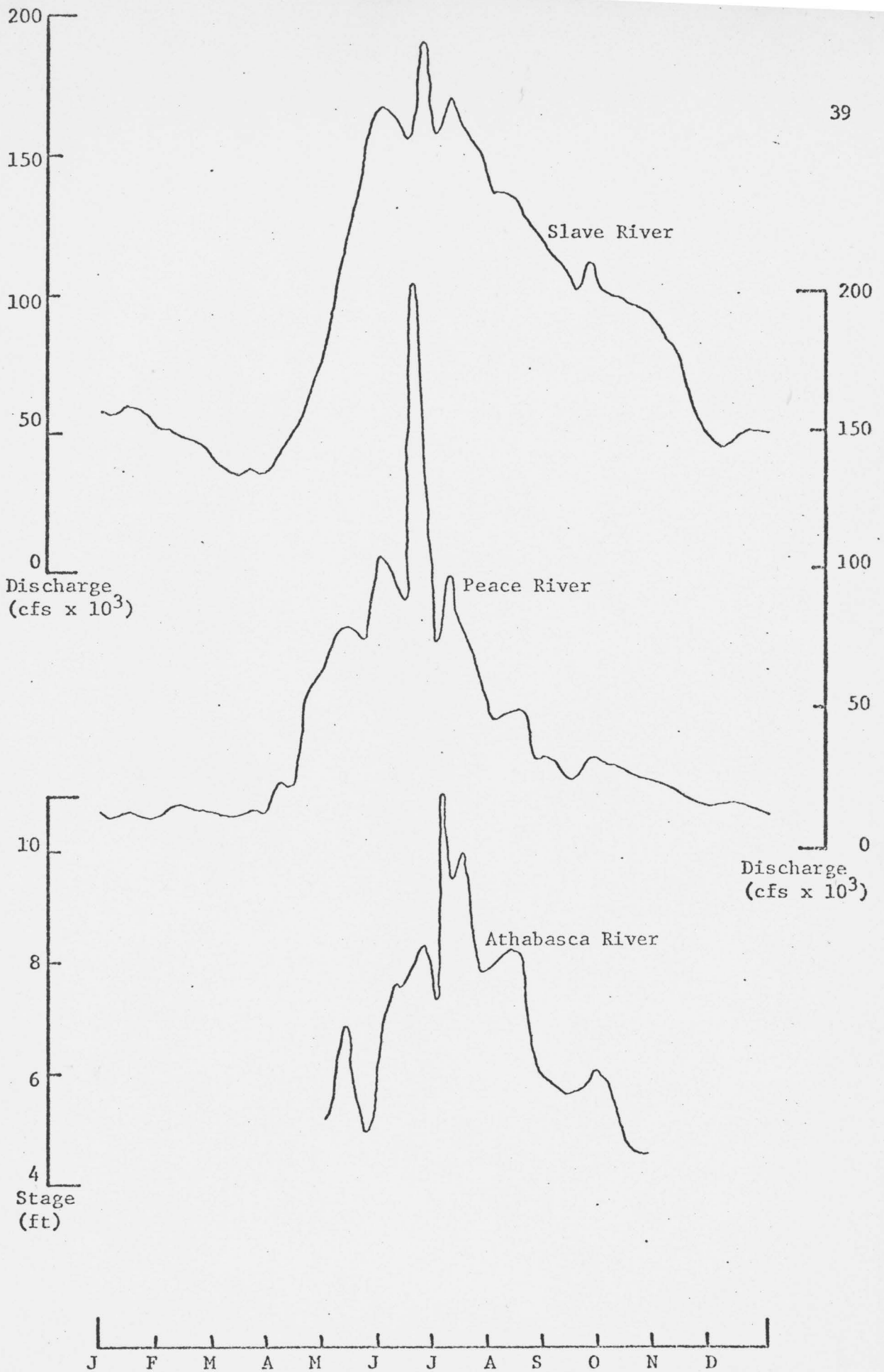


Figure 9. Hydrographs of the Slave, Peace and Athabasca Rivers for 1968.

Slave River

	Discharge	Ca <sup>++</sup>	pH	SATCAL	SO <sub>4</sub> <sup>--</sup>
Discharge	1.00	0.25	-0.24	0.33	0.50
Ca <sup>++</sup>		1.00	0.05	0.47	0.80
pH			1.00	0.71	-0.43
SATCAL				1.00	0.15
SO <sub>4</sub> <sup>--</sup>					1.00
log (discharge)	-	0.13	-0.24	0.29	0.42

5% significance value = 0.60

Peace River

	Discharge	Ca <sup>++</sup>	pH	SATCAL	SO <sub>4</sub> <sup>--</sup>
Discharge	1.00	-0.35	-0.41	-0.27	0.11
Ca <sup>++</sup>		1.00	0.59	0.68	0.61
pH			1.00	0.93	-0.15
SATCAL				1.00	0.03
SO <sub>4</sub> <sup>--</sup>					1.00
log (discharge)	-	-0.50	-0.56	-0.39	0.10

5% significance value = 0.58

Table 3. Simple correlation matrices for Slave River at Fort Fitzgerald and Peace River at Peace Point in 1968.

SATCAL and between Ca and  $\text{SO}_4$  the table above suggests that both sulfate and carbonate equilibria are important in the Peace River, whilst either carbonate equilibrium in the Slave River is subordinate to the sulfate equilibrium process or the increase of  $\text{Ca}^{++}$  in the Slave River is derived mainly from inputs of gypsum in solution, phenomena which possibly reflect the increased inputs of gypsum derived streams to the Slave River

## 2. The Salt River area

Hydrologically the Salt River is in marked contrast with the Peace River and Slave River system. It rises from a series of lakes on the plateau and passes into the Slave River valley at a point where the escarpment decreases in height. The river flows along the valley parallel to the Slave River at the base of the scarp and is fed by a number of tributaries rising from the scarp foot. Benchmark Creek is typical of these tributaries, having a high dissolved solids content but with no discrete rising. The hydrograph for Benchmark Creek shows that it ceases to flow from December through April, and has a distinct peak flow in early May which is a result of snowmelt in the creek basin. Following this peak the flow declines rapidly with a few minor peaks, attributed to rainstorms.

The Water Survey of Canada maintained a V-notch weir on Benchmark Creek from March to December 1968, at which time it was destroyed. Daily discharge records exist for this period. In addition, regular water samples were taken every month from August to December at the weir site. This is the only site within Wood Buffalo National Park having both discharge and concentration data, and is therefore used as a basis for the

following analysis. The records for the period August - December 1968 are sufficient to demonstrate that the concentration of  $\text{Ca}^{++}$ ,  $\text{SO}_4^{--}$ ,  $\text{Cl}^-$  and  $\text{HCO}_3^-$  is dependent on discharge during the September rise (Figure 10). pH shows a partial response, but appears to damp the effects of a falling stage. This last effect is responsible for the lack of a simple relationship between SATCAL and discharge. (In the case of SATGYP, pH does not enter into the index and there is an inverse linear relationship between this index and  $\log(\text{discharge})$ , shown in Figure 11). It is possible that the pH lag effect is consequent upon absorption of positive ions onto clay particles with preferential absorption of  $\text{H}^+$ . With a higher than normal flow, concentrations decrease leading to desorption, followed by preferential absorption of  $\text{H}^+$  as the stage falls and concentrations increase. The fact that all ions appear to react in a similar manner to changes in discharge suggest that the determining factors are the hydrologic conditions within the zone or rock-water interaction.

Data in this area is insufficient to allow any hypotheses to be tested statistically; but some inferences may be drawn from the local area pattern of chemical variables. Since Benchmark Creek ceases to flow for an appreciable period it is difficult to make any distinction between groundwater flow and direct runoff (cf. Pinder and Jones). If indeed the maximum concentrations correspond to base flow (assuming this to be solely groundwater), then the concentration of this groundwater is extremely high, being of the order of 19,000 ppm  $\text{Cl}^-$ , 12,600  $\text{Na}^{++}$ , 2,600 ppm  $\text{SO}_4^{--}$ , 1000 ppm  $\text{Ca}^{++}$ , 280 ppm  $\text{HCO}_3^{--}$  and pH 7.2. Representative values for the various sites in late May are given below:

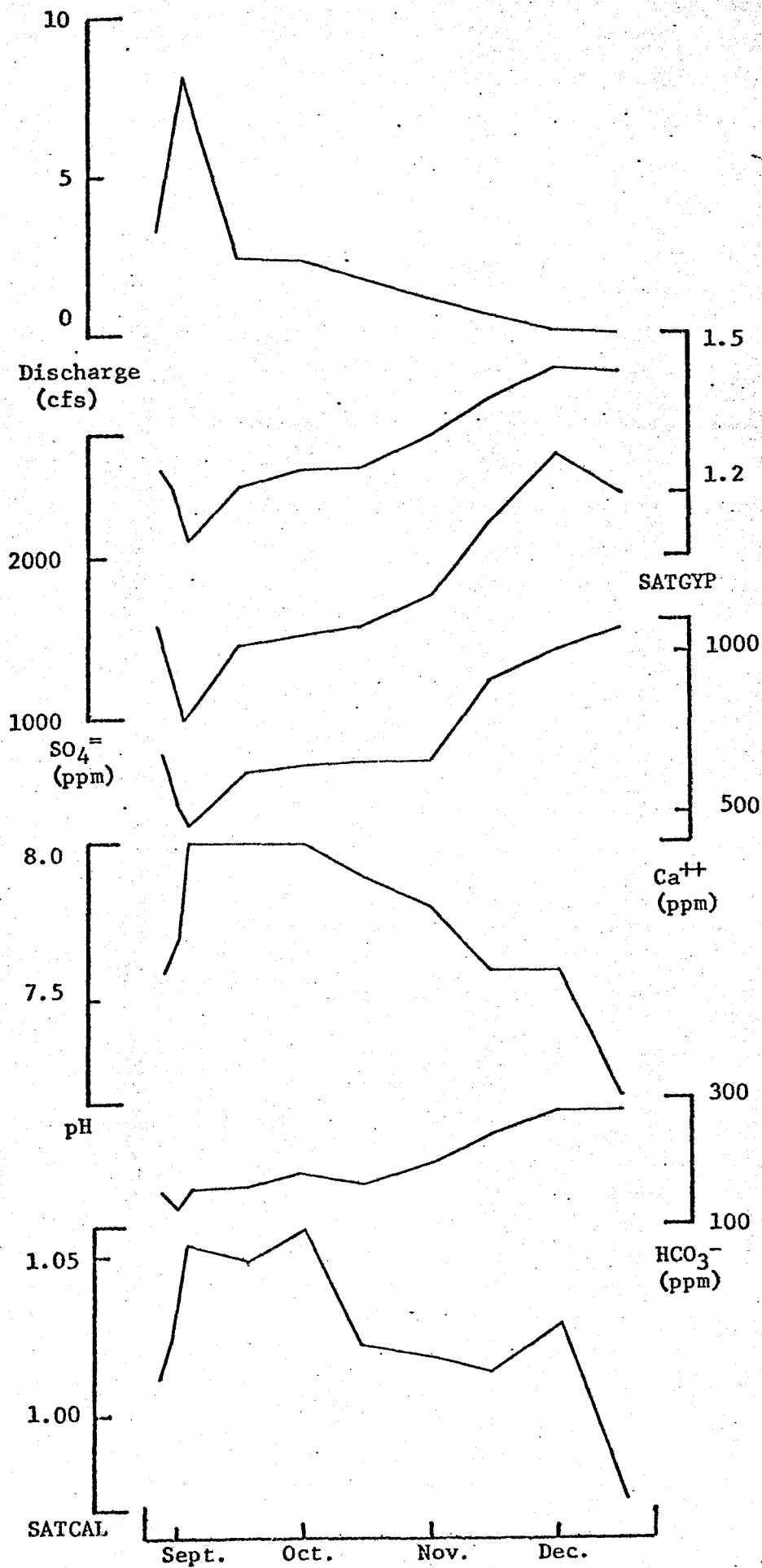


Figure 10. Summary data for Benchmark Creek, 1968.

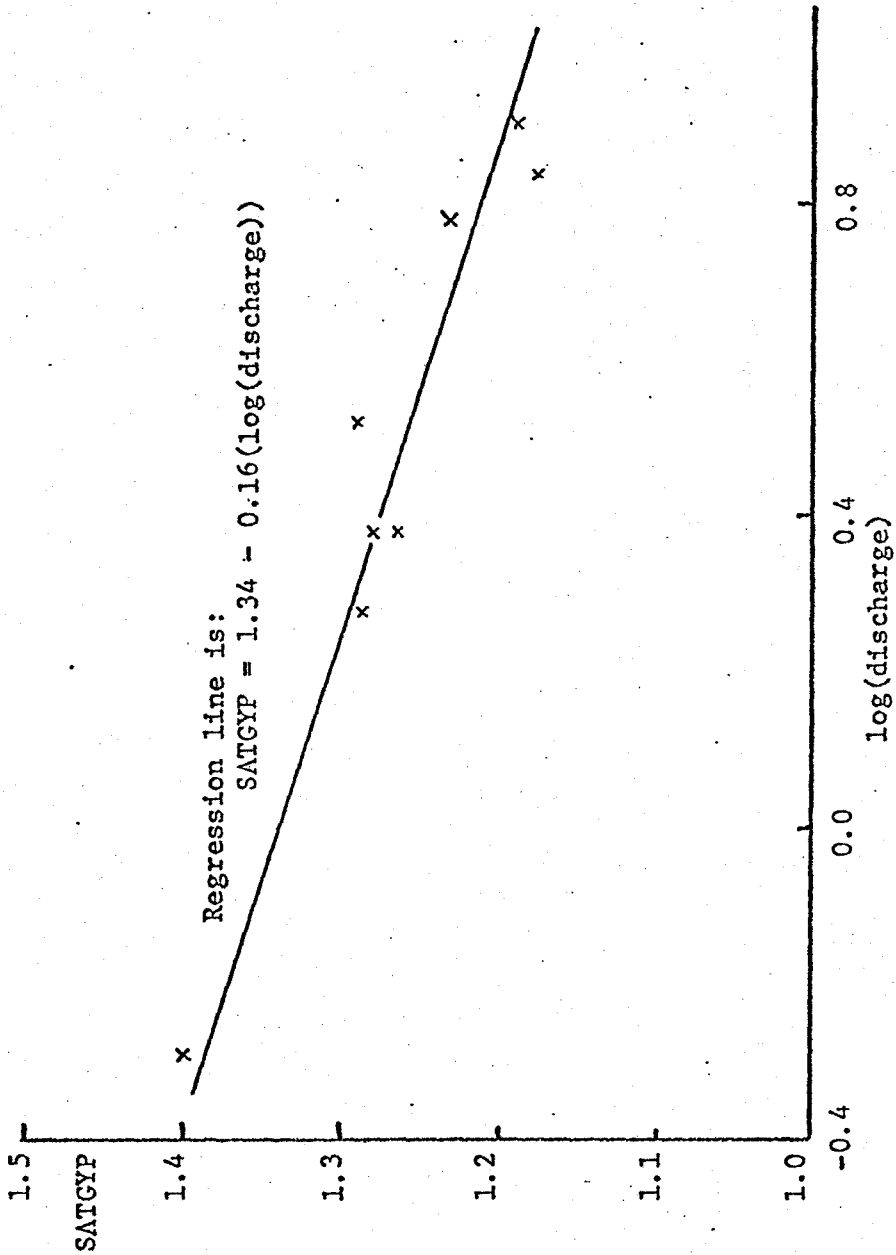


Figure 11. Regression of discharge and SATGYP for Benchmark Creek, for the period Sept.- Dec. 1968.  
 $r = 0.83$ , indicating the relationship to be significant at the 0.01 level.

(Only ions pertinent to this discussion are listed:)

	<u>Cl<sup>-</sup></u> (ppm)	<u>Ca<sup>++</sup></u> (ppm)
Salt River, above Benchmark Creek	800	172
Benchmark Creek	4100	516
Salt River, below Benchmark Creek	1225	208
Cave IC3 (see figure 5 )	1075	460
Cave IC4 (see figure 5)	1050	372
Spring above Salt River	1125	276
Little Buffalo River at falls	7.6	176
Slave River	9.1	29
Peace River	2.2	33

Brandon quotes the composition for the Little Buffalo River below the scarp as:

	pH	Ca	Mg	Na	HCO	SO <sub>4</sub>	Cl
August 61	7.5	549ppm	31.3ppm	262ppm	128ppm	124ppm	124ppm

The Salt River area nowhere exhibits concentrations as great as those suggested for groundwater by the Pinder and Jones method. The flow of Benchmark Creek in May is some 100 times greater than that corresponding to the maximum chemical load, whilst the Cl<sup>-</sup> content is 5 times less than the maximum. Shallow groundwater, as sampled in the caves and which rises in the springs has a Cl<sup>-</sup> content  $\frac{1}{4}$  of that of Benchmark Creek, but 50% greater than Salt River. Partial analyses of three sinkhole lakes are:

	<u>Cl<sup>-</sup></u> ppm	<u>Ca<sup>++</sup></u> ppm	<u>SO<sub>4</sub><sup>=</sup></u> ppm
Pine Lake	4.2	52.8	12
SH to S of Pine Lake	3.6	76.4	16
Nyarling Wdn. SH	3.5	74.0	52

There appears to be a clear division between groundwater flow and surface or subsurface flow networks. Salt River is fed by tributaries similar to Benchmark Creek below the escarpment, but has a much larger surface component at the confluence than does Benchmark Creek. This is

to be expected since Benchmark Creek is fed exclusively by seepage from below the escarpment and has only a small catchment in the classical sense. The network intersected by the caves in the Salt River area seems to be only a local development in response to the fracturing and the transection of the folded zone by the Salt River. The Nyarling Warden sinkhole is 180' deep and would intersect such a network if it were common to the whole area. It is evident from the analysis (vs) that it corresponds closely to the sinkholes in other areas in Wood Buffalo National Park.

The presence of large amounts of  $\text{Cl}^-$  and  $\text{Na}^+$  in Benchmark Creek serves to depress the thermo-dynamic concentrations of other ions. A comparison of the plots of SATGYP and SATCAL against  $\text{Ca}^{++}$  illustrates the necessity of considering activity coefficients in such a situation. At no time is Benchmark Creek saturated with gypsum, whilst if the presence of  $\text{Na}^+$  and  $\text{Cl}^-$  is ignored it is always supersaturated. A consideration of Zverev's  $(\text{Ca}^{++}):(\text{SO}_4^{=})$  ratio yields the results:

<u>site</u>	<u><math>(\text{Ca}^{++})/(\text{SO}_4^{=})</math></u>
Benchmark Creek	1.2
Salt River	1.1
Little Buffalo River	6.5
Slave River	2.9
Peace River	2.5

Zverev's scheme is stated to apply to subsurface waters, and it is only Benchmark Creek which approximates this requirement. Both Benchmark Creek and the Salt River, which is largely fed by tributaries similar to it, fall into Zverev's category of  $\text{Ca}^{++} \approx \text{SO}_4^{=}$ , indicating that these flows originate from a zone of intense water exchange in areas of gypsum and anhydrite. The other three rivers fall into the  $\text{Ca}^{++} > \text{SO}_4^{=}$  category, which according to Zverev indicates the presence of organic reducing

processes. In this particular instance, however, the scheme is not applicable since all three rivers are mostly fed by water from outside the gypsum area, and the chief controlling factor is the relative availability of  $\text{Ca}^{++}$  and  $\text{SO}_4^{=}$  ions. The upper reaches of the Peace and Athabasca Rivers (which combine to form the Slave River) flow over extensive carbonate deposits, and much of the Little Buffalo River flows over carboniferous strata and drift.

## CHAPTER FOUR

### THE CANAL FLATS AREA

#### I. DESCRIPTION

##### 1. Geology and morphology

The location of the area is shown in Figure 12. Local relief along the Lussier River to the east of the Hughes Range (above the Lussier Canyon) is 3500 feet and Coyote Creek is separated from the Lussier River by a 2500 feet divide. The Hughes Range forms the most westerly range of the Rocky Mountains, lying immediately to the east of the Rocky Mountain Trench in which the Lussier River flows south to join the Kootenay River.

Figure 13 shows the study area in more detail; the Lussier River and Coyote Creek are the only perennial streams. Part of the area was described by Leech (1954). This is the only geologic information available. He describes the Lussier River-Coyote Creek area south of Alces Lake as a graben-type structure with limestones, shales and gypsum of Mississippian and Silurian age (dipping at about  $12^{\circ}$  between north-east and south-east) down faulted into the Cambrian and Ordovician strata dipping at  $50^{\circ}$  -  $60^{\circ}$  to the east (Beaverfoot Formation, McKay Group and the Jubilee Formation) which form the Hughes and Van Nostrand Ranges to the west and east. Both river valleys are thickly covered with

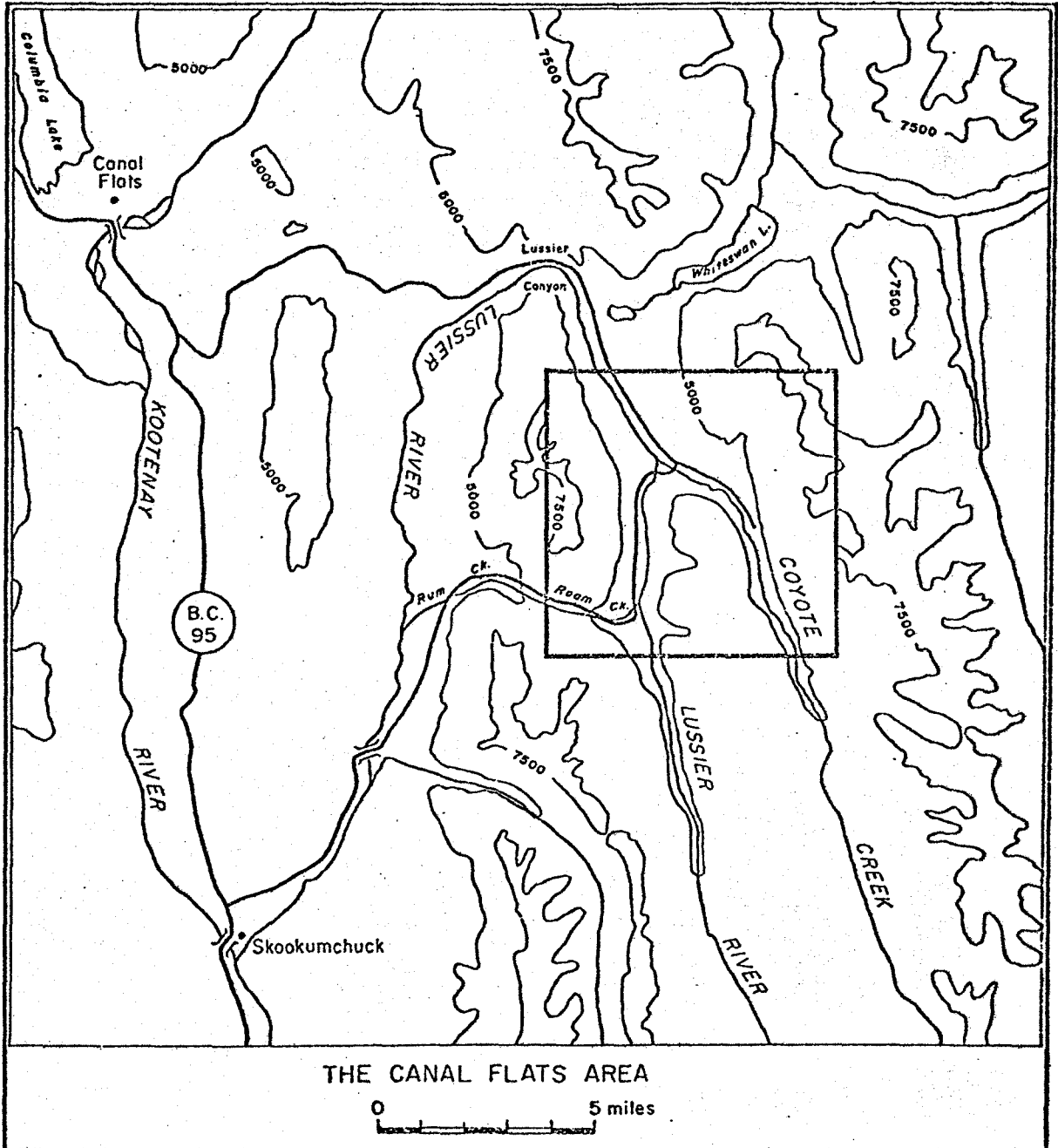


Figure 12.

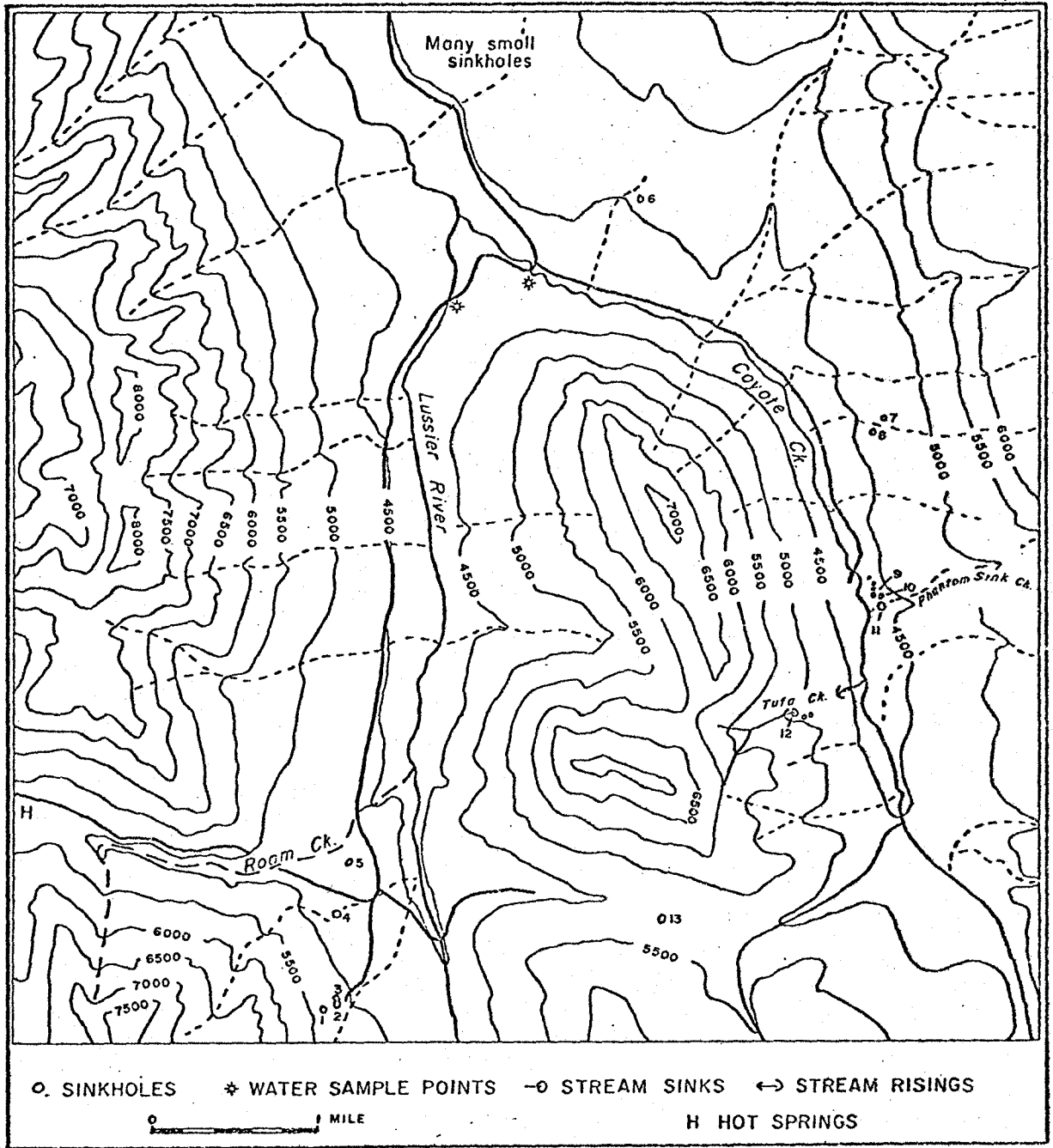


Figure 13. The Canal Flats study area.

Wisconsin drift to an altitude of about 5500' and erratics found at the head of Ram Creek suggest that the whole area has been glaciated. Leech considers that the drift in the upper Lussier River is possibly a result of ponding until flow began through what is now the Lussier Canyon.

The drift cover obscures all but the uppermost stratum of the graben and exposures of the gypsiferous strata are thus rare.

Two lithologic units are contained within the Silurian and/or Devonian, but their relationship cannot be determined as they are nowhere seen in contact. One, consisting of gypsum and limestone, is exposed in some five places in the upper Lussier and Coyote valleys. Leech quotes no dip or strike measurements but considers that the beds in the largest exposure, (on the east bank of the Lussier River 1 mile above Roam Creek, shown in Plate 5), may strike north-east and dip steeply south-east. The exposures are varied in lithology but are described as predominantly gypsum with impurities of anhydrite and calcium and magnesium carbonates. In all cases the impurities occur as discreet laminae.

## 2. Karst features

### a) Sinkholes

The sinkholes concerned in this study are shown in Figure 13. In only one case is the bedrock exposed (Plate 6). Other similar cases reported by Leech could not be located either from the air or in the field. Leech assumed that all sinkholes were an indication of underlying gypsum, but pointed out that they may develop in other circumstances:

".....although sinkholes are important indicators of gypsum they are not infallible guides. They can develop entirely in glacial silts, and they occur above fault breccia north of White Swan Lake. They are probably most reliable as guides when they are closely spaced, as they are near the east edge of the map-area between Coyote Creek and White Swan Lake".



Plate 5. The gypsum exposure on the Lussier River.



Plate 6. The gypsum exposure in sinkhole 1. View to north.

The sinkholes in the north-east of the area are all small (maximum diameter is  $\sim 30'$ ), none contain water and all are covered in bush. If they are presently active their rate of expansion must be so slow that vegetation can rapidly colonize any fresh exposures of till formed by collapse. They are integrated with a fossil surface drainage network in that the smaller ones occur in the floors of abandoned channels, which terminate in the larger sinkholes. In the rest of the area the sinkholes are much larger (Plates 7 and 8) and most contain water. All are developed in thick drift. They appear to be expanding because there is little vegetative cover on their sides, and trees that have fallen into them lie directly down gradient.

A more detailed analysis of the distribution of sinkholes in the Lussier River - Coyote Creek area is given below, but the main feature of the distribution is that all are developed close to tributary valleys to the main rivers (Figure 13), with the exception of the one in the col to the east of Roam Creek.

b) Other karst features

Another feature reported in the area by Leech is a sinking stream:

"In Coyote Creek valley a creek disappears down a sinkhole and reappears at the gypsum outcrop half a mile away".

This is believed to be the stream shown on Figure 13 as Phantom Sink Creek. It does not in fact sink, but flows through a degraded sinkhole and continues as a surface stream to join Coyote Creek just to the south of the outcrop mentioned by Leech. Although this stream does not sink, another nearby stream, Tufa Creek, sinks in a large sinkhole of an altitude of 5000 feet, and rises at several points at about 4600 feet. The streams below the resurgences are actively depositing a low density,

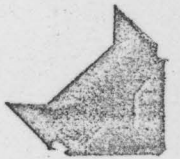
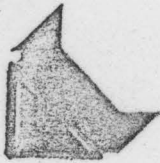
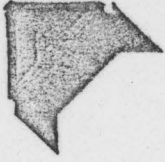


Plate 7. Aerial view of sinkhole 5. The land drain enters the sinkhole from the left of the photograph.



Plate 8. Aerial view of sinkholes 7 (top) and 8, from the south.

spongy tufa which hardens on exposure to the atmosphere.

Thermal springs in the area have been described by van Everdingen (1969) and shown to be associated with major faults. Their overall chemical composition indicates that they do not form a part of the local groundwater flow network, but are rather isolated features emanating from deep endogenic sources. Interestingly, however, calculations show that the saturation indices with respect to gypsum and calcite are comparable to those for the surface streams in the area (Table 4).

### 3. Field program

As in Wood Buffalo National Park the field program in Canal Flats was specifically aimed at an integrated geochemical and hydrological study of the karst groundwater system. Those sinkholes containing groundwater were studied in detail, and an overall view of the regional pattern was derived from a study of Coyote Creek, the Lussier River, and the Lussier River below the confluence with Coyote Creek.

Routine sampling sites are shown on Figure 13. Depth samples were taken in sinkholes 5, 9 and 10. These are the only sites to show significant penetration of the groundwater zone. Tufa Creek was sampled above and below the underground section, and a dye trace was attempted to give an estimation of flow through time. The test<sup>1</sup> location is shown in Figure 15(a). No positive result was obtained, possibly due to the presence of a large amount of clay minerals in suspension in the rising pools. The dye used was fluorescein, and it is known that this dye is subject to considerable adsorption on clay minerals. It is also

---

<sup>1</sup>Charcoal detectors were eluted with a KOH/methanol solution, and this ellutrient tested on a Fisher III fluorometer.

Table 4. Chemical parameters of hot springs in the Canal Flats area. Adapted from van Everdingen (1969), Tables 2 and 3.

Site	T°C	pH	Analyses reported in ppm								SATDOL		
			Ca <sup>++</sup>	Mg <sup>++</sup>	Na <sup>+</sup>	K <sup>+</sup>	HCO <sub>3</sub> <sup>-</sup>	SO <sub>4</sub> <sup>=</sup>	Cl <sup>-</sup>	H <sub>2</sub> S	SATCAL	SATGYF	
Lussier Canyon spring	43.4	7.1	145	25	875	10	218	135	1402	0.5	1.02	0.99	0.77
Ram Creek spring	34.6	7.6	50	15	2.6	1.3	155	57	1.7	0	1.02	1.00	0.77

The saturation indices given here are those used throughout this thesis. These, rather than those used by van Everdingen, are used to maintain uniformity.

difficult to detect under field conditions as it fluoresces in the same spectral band as Chlorella, which is present in all natural waters.

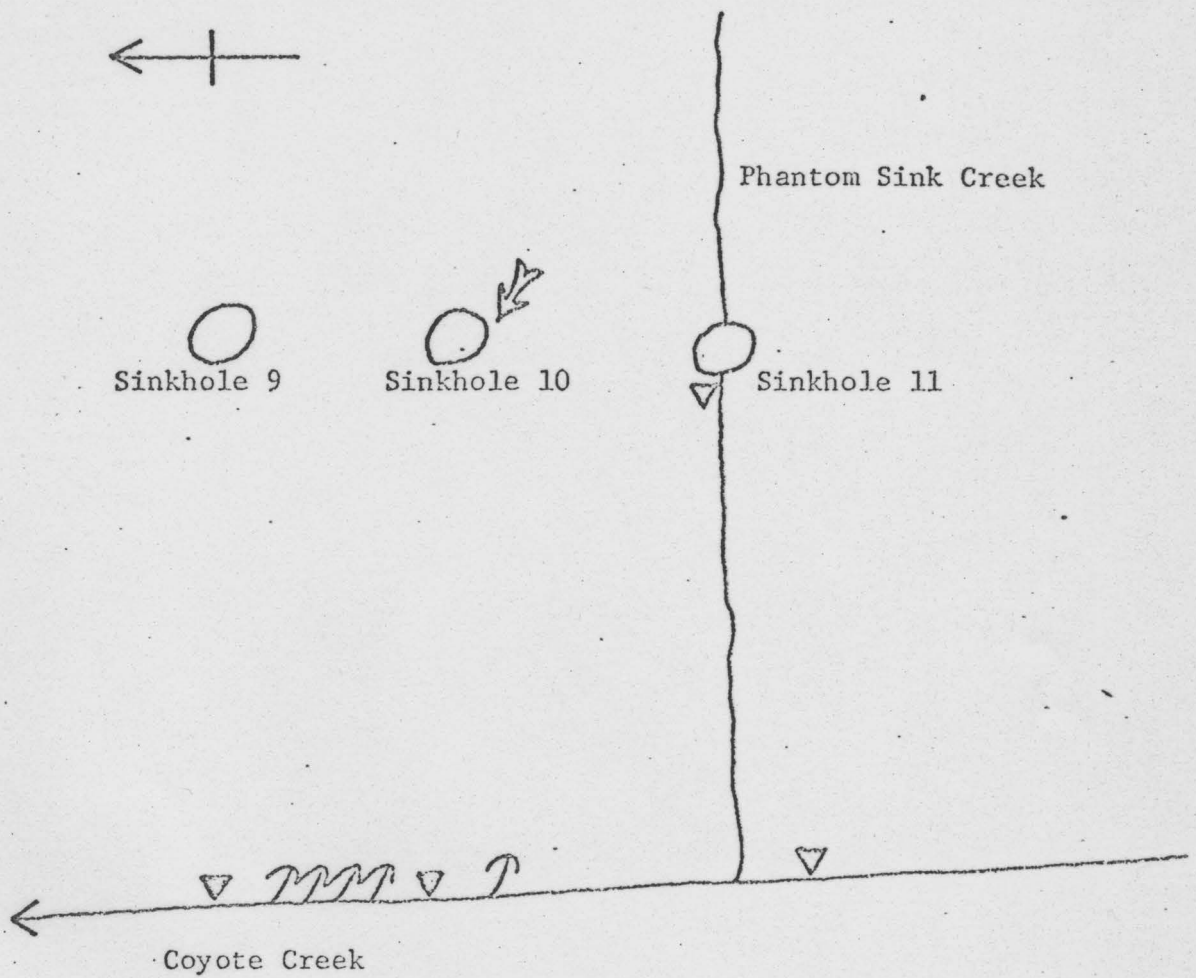
A second dye trace was performed in the Phantom Sink Creek area, and is shown schematically in Figure 14. The dye was injected into sinkhole 10 and rapidly appeared 50 feet away in sinkhole 9, indicating an intimate connection between the two. A positive trace was established from these sinkholes to a number of small risings appearing in till immediately above Coyote Creek about 200' downstream of the confluence of Phantom Sink Creek. These springs are  $1/3$  mile from the sinks and 150 feet lower in altitude. The flow through time was between four and ten days. The rapid flow time between the two sinkholes, plus the fact that the water in each is at the same level<sup>1</sup> indicates that they are connected via the groundwater system, and that an ordering of flow paths exists between them.<sup>2</sup> This groundwater connection makes it valid to regard samples taken from such sinkholes as indicative of conditions in the groundwater system.

There is no evidence of any channelled surface flow into the sample sinkholes except for sinkhole 5. This, the largest of all (1000' in circumference, Plate 6), is used as a land drain for roads constructed by the lumber operation in the Lussier River area. The water is consequently very silty, and the bottom of the sinkhole is unconsolidated mud. The effect of surface runoff is shown by the variation in water height:

---

<sup>1</sup>The section was surveyed by 100' steel tape and Suunto compass, clinometer to an accuracy of  $\pm 5$ .

<sup>2</sup>This ordering may take the form of discrete pipe development, rather than diffuse flow.



- ⤿ 5lbs. fluorescein injected
- ▽ Detectors (no result)
- ▽ Detectors (showed positive result 10 days after injection)
- ⤿ Springs

Figure 14. Dye test on east side of Coyote Creek.

<u>date</u>	<u>stage</u>	<u>change</u>
16 July	5 <sup>1</sup> / <sub>4</sub> "	
		6 <sup>5</sup> / <sub>16</sub> "
23 July	11 <sup>9</sup> / <sub>16</sub> "	

During the same period no change was observed in any of the other sinkholes. The water in sinkhole 5 is also markedly warmer than elsewhere, suggesting that groundwater plays a minor part in the regime of this feature. The significance of this sampling site is consequently doubtful.

## II. GEOMORPHOLOGICAL IMPLICATIONS OF THE HYDRO-CHEMICAL STUDY

The sampling net has been described above (vs Chapter III, part I). Table 5 summarizes the analyses.

Sample sites fall into three groups: major streams, sinkhole water and Tufa Creek. Certain characteristics of these groups can be seen from the table:

- a) Tufa Creek samples have a markedly higher value for  $\text{Ca}^{++}$  than either of the other groups
- b)  $\text{Ca}^{++}$  values for sinkhole waters and the two major streams are similar
- c)  $\text{HCO}_3^-$  values for Tufa Creek and sinkhole waters are similar, and are greater than those for the major streams.

Apart from Tufa Creek, the  $\text{Ca}^{++}$  values are comparable with those obtained from limestone karst areas elsewhere in the Canadian Rockies, where it is generally possible to distinguish a three zone pattern of:- surface runoff above the treeline (where  $\text{Ca}^{++}$  ranges from 0-50 ppm.), surface runoff below the treeline ( $\text{Ca}^{++}$  = 50-100 ppm.) and true groundwater flow ( $\text{Ca}^{++}$  = 100-175 ppm.).

This would indicate that, with the exception of Tufa Creek, the groundwater network is largely developed in calcareous materials. The gypsum areas as defined by Leech form only a small proportion of the Lussier basin above the hot springs and it is thus to be expected that the main regional controls of chemical solution would be those exerted by the limestone process.

Saturation values with respect to calcite and gypsum are also

Table 5. Summary data for Canal Flats area.

Site	Date	°C Temp	pH	ppm CaCO <sub>3</sub>			ppm		Ion balance error	Ca:Mg	SATCAL		SATGYP		Ca:SO <sub>4</sub>
				Ca <sup>++</sup>	Mg <sup>++</sup>	HCO <sub>3</sub> <sup>-</sup>	SO <sub>4</sub> <sup>=</sup>	CO <sub>2</sub>			SATDOL	SATDOL			
Lussier River in the Lussier Canyon	15/6	9.0	8.35	137	60	137	-	7.5	-	2.3	1.05	1.00	-	-	
	20/6	10.0	8.45	103	68	130	-	5.0	-	1.5	1.06	1.05	-	-	
	23/6	6.2	8.70	120	68	116	-	5.0	-	1.8	1.08	1.05	-	-	
	16/7	10.6	7.60	205	68	190	76	10.0	7.2	3.0	1.01	0.96	0.74	2.6	
Coyote Creek at bridge	22/6	6.5	7.82	120	34	130	36	10.0	19.7	3.5	0.97	0.93	0.70	3.2	
	23/6	5.6	7.95	120	51	137	-	10.0	-	2.4	0.99	0.96	-	-	
	16/7	9.7	8.65	137	68	204	48	10.0	14.5	2.0	1.12	1.08	0.71	2.7	
Lussier River at bridge	22/6	7.0	8.10	103	51	103	60	10.0	14.7	2.0	0.98	0.96	0.71	1.6	
	23/6	5.6	8.65	103	68	116	-	5.0	-	1.5	1.06	1.04	-	-	
	16/7	10.3	8.20	171	86	136	60	5.0	31.9	2.0	1.06	1.04	0.73	2.7	
Tufa Creek (sink area (see fig. 15 for locations)	(rising 1	19/6	4.0	8.40	223	85	260	60	15.0	22.8	2.6	1.11	1.06	0.74	3.6
	(rising 2	21/6	4.9	7.28	1250	188	233	1150	40.0	4.5	6.6	1.06	0.99	1.01	1.0
	(stream	21/6	5.0	7.35	1113	117	240	908	35.0	7.9	9.5	1.07	0.99	0.99	1.2
		21/6	7.9	8.40	1130	86	205	1070	30.0	-0.1	13.1	1.23	1.13	1.00	1.0
Lussier R./ Roam Creek area	(ck. to SH5	22/6	19.8	8.50	103	51	240	-	15.0	15.0	2.0	1.12	1.10	-	-
	(SH 5	22/6	18.0	8.45	137	51	205	16	15.0	22.0	2.7	1.12	1.09	0.67	8.2
	(SH 5	16/7	16.4	7.60	137	68	204	4	10.0	31.0	2.0	1.01	0.98	0.61	32.9
	(SH 5	23/7	17.9	8.00	137	68	239	0	15.0	25.9	2.0	1.05	1.03	-	-
	(SH 5, base	23/7	14.6	7.80	120	103	273	8	15.0	20.7	1.2	1.02	1.02	0.63	14.4
	(SH 4	22/6	17.5	8.40	103	85	158	-	15.0	-	1.2	1.08	1.08	-	-
	(SH 2	24/7	15.7	7.90	68	17	120	24	10.0	0.4	4.0	0.95	0.91	0.67	2.7
	(SH 3	24/7	14.6	8.20	137	51	205	32	15.0	15.9	2.7	1.05	1.01	0.70	4.1

continued

Table 5. continued

Site	Date	°C Temp	pH	ppm CaCO <sub>3</sub>			ppm			Ion balance CO <sub>2</sub> error	SATCAL		SATGYP		Ca:SO <sub>4</sub>
				Ca <sup>++</sup>	Mg <sup>++</sup>	HCO <sub>3</sub> <sup>-</sup>	SO <sub>4</sub> <sup>=</sup>	CO <sub>2</sub>	Ca:Mg		SATDOL	SATGYP			
East side ( SH 8	21/6	15.8	7.75	137	51	164	24	15.0	27.0	2.7	1.01	0.99	0.68	5.5	
of Coyote ( SH 9	19/6	12.0	7.90	120	51	164	40	10.0	16.0	2.4	1.01	0.99	0.70	2.9	
Creek ( SH 9	23/7	12.6	7.45	154	68	183	44	20.0	17.0	2.3	0.97	0.94	0.71	3.4	
( SH 9, base	23/7	6.2	7.40	222	68	222	124	25.0	16.6	3.3	0.96	0.92	0.78	1.7	
( SH 10	19/6	14.0	7.95	137	34	192	44	10.0	9.2	4.0	1.04	1.00	0.71	3.0	
( SH 10	23/7	13.9	7.70	137	51	188	24	20.0	22.1	2.7	0.98	0.95	0.68	5.5	
( SH 10, base	23/7	6.8	7.25	735	51	222	556	25.0	6.5	14.4	1.03	0.95	0.93	1.3	
( SH 11	19/6	7.8	8.55	86	68	144	32	10.0	18.4	1.3	1.05	1.03	0.68	2.6	
( risings	21/6	7.0	7.80	103	0	123	64	10.0	-10.2	-	0.96	-	0.72	1.5	

Ca<sup>++</sup>, Mg<sup>++</sup>, HCO<sub>3</sub><sup>-</sup> expressed as ppm CaCO<sub>3</sub>

SO<sub>4</sub><sup>=</sup> expressed as ppm SO<sub>4</sub><sup>=</sup>

CO<sub>2</sub> expressed as ppm CO<sub>2</sub>

Ca<sup>++</sup>:Mg<sup>++</sup> expressed as Mg<sup>++</sup> = 1.0

Temperature in degrees centigrade

SATCAL is index of saturation with respect to calcite

SATDOL " " " " " " " dolomite

SATGYP " " " " " " " gypsum

Ca<sup>++</sup>:SO<sub>4</sub><sup>=</sup> expressed as SO<sub>4</sub><sup>=</sup> = 1.0

shown in Table 5. These illustrate the above point in that the values of SATGYP for river and sinkhole waters show considerable undersaturation: those for SATCAL approximate saturation. The only group of samples to show oversaturation with respect to gypsum is the Tufa Creek series. Here, the analysis of water flowing into the sinkhole near the head of the valley is comparable to those for other streams and sinkholes in the Canal flats area. The resurgant water has values of SATGYP of 0.99-1.0, suggesting that this is the only flow to intersect a large gypsum deposit (Figure 15a). The only other known subsurface flow to be investigated is that from sinkholes 9 and 10 to the rising by Coyote Creek (Figure 15b). The water throughout this system shows approximate saturation with respect to calcite, but marked undersaturation with respect to gypsum with one exception. The depth sample in sinkhole 10 shows higher values for  $\text{Ca}^{++}$ ,  $\text{SO}_4^-$  and SATGYP than any sites other than Tufa Creek. It is difficult to reconcile the analysis for the bottom of sinkhole 10 with the other analyses in this area as the ion balance error is similar, suggesting that measurement error is unlikely to be wholly responsible for the discrepancy. It may be that the extreme low point of this sinkhole represents a static reservoir below any flow paths into or out of it. The low value of SATGYP for the rising contrasts with that for the Tufa Creek risings. The length of the direct underground flow path in the Sinking Creek area is  $1/4$  of that of Tufa Creek, but SATGYP shows only an insignificant rise between the surface of the water in sinkholes 9 and 10 and the rising, suggesting that the flow is not through gypsiferous strata or till.

The calcium:magnesium ratios show one significant trend - at high

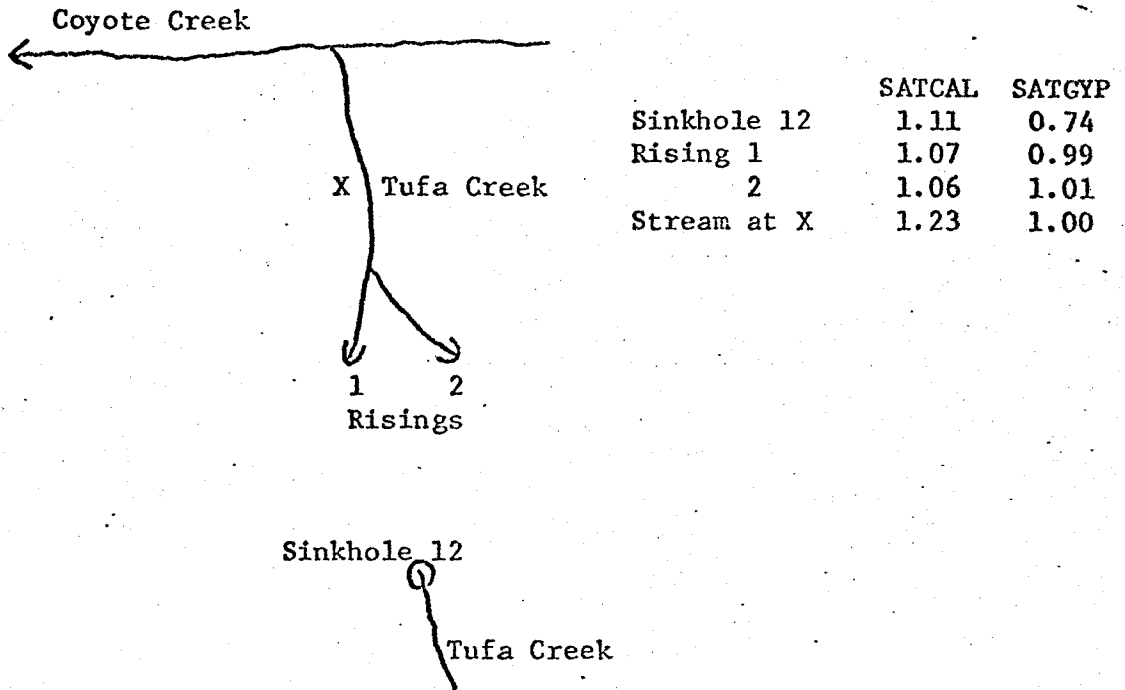


Figure 15a) summary of hydro-chemical data for Tufa Creek area.

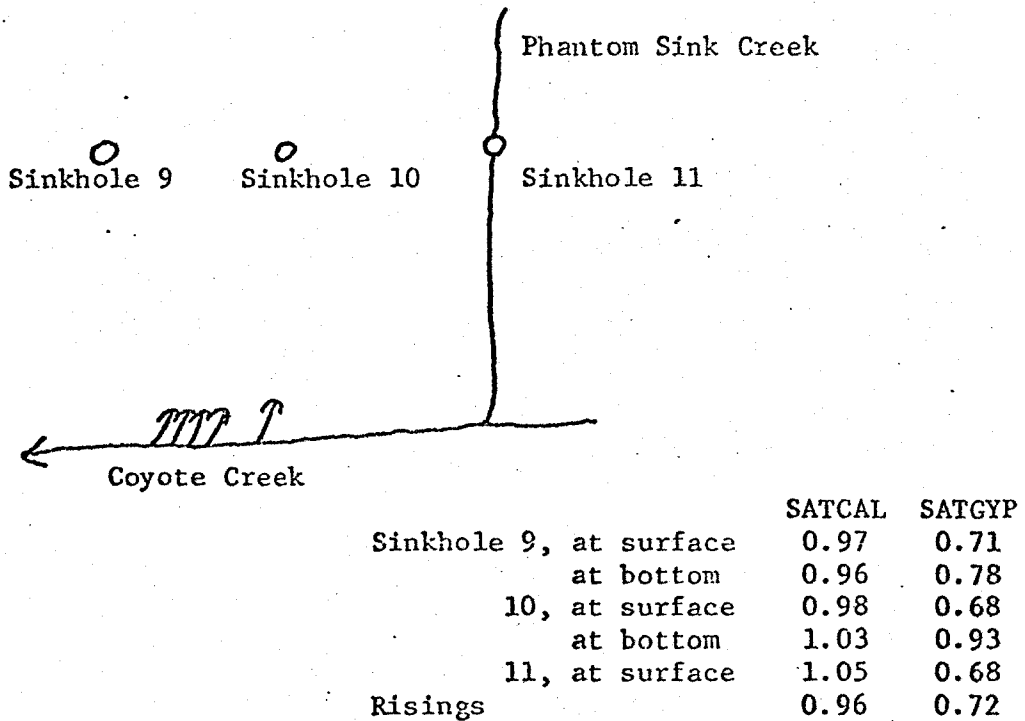


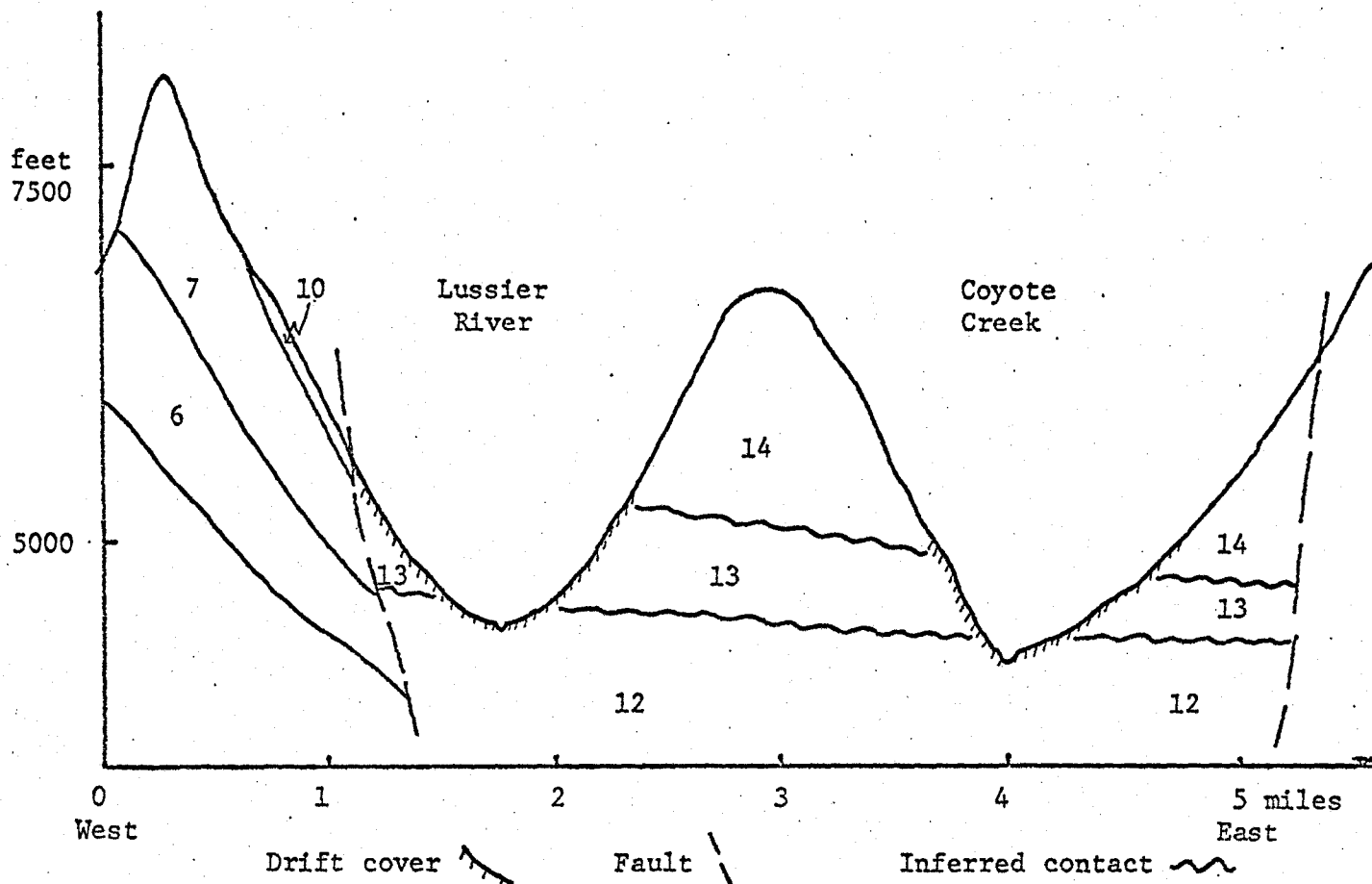
Figure 15 b) summary of hydro-chemical data for Phantom Sink Creek area.

values of  $\text{SO}_4^{=}$  the ratio is considerably greater than the norm of 1.5 - 2.5. In the Tufa Creek area the ratio rises from 2.6 to 6.6 and 9.5 between sink and risings, increasing again to 13.1, the second highest value in the whole study area, some 500' below the risings. The highest value is 14.4 for the bottom of sinkhole 10 in the Sinking Creek area. The lack of correspondence between increasing  $\text{SO}_4^{=}$  and relative abundance of  $\text{Mg}^{++}$  suggests that the source of sulfate ions is divorced from that of  $\text{Mg}^{++}$  ions. As the index SATDOL shows approximate saturation for all samples and parallels the trends in SATCAL the sources of magnesium and calcium appear to be the same. The geologic cross-section of the Lussier River and Coyote Creek valleys (Figure 16) suggest that much of the area is underlain by dolomitic strata of the Devonian era, Brisco series, reinforcing the conclusion that  $\text{Mg}^{++}$  is present as dolomite (and that epsomite ( $\text{MgSO}_4 \cdot 7\text{H}_2\text{O}$ ) is not present within the gypsum deposits). Data from elsewhere in the Rocky mountains usually shows that in areas of limestone the Ca:Mg ratio is generally greater than 4:1, and in an area of dolomite on the Niagara Escarpment (Ontario) ratios are of the order of 2:1.

#### Sinkhole genesis and distribution and groundwater flow patterns

The distribution of sinkholes within the Canal Flats area cannot be completely explained in the absence of detailed geologic data. No apparent ordering exists in the distribution in the main Coyote Creek - Lussier River area, but all except sinkhole 5 have developed in proximity to subsidiary valleys. The presence of stratum 12 in the position shown in Figure 16 is inferred from the small exposures mapped by Leech, by the conclusion

Figure 16. Geologic cross-section of the Canal Flats area.



Mississippian

14 - limestones, shales, chert

Silurian or Devonian

13 - gypsum, limestone

12 - dolomite, limestone, shale

Upper Ordovician

10 - Beaverfoot Fm., dolomite, limestone

Upper Cambrian / Lower Ordovician

7 - McKay Group, limestone, shale

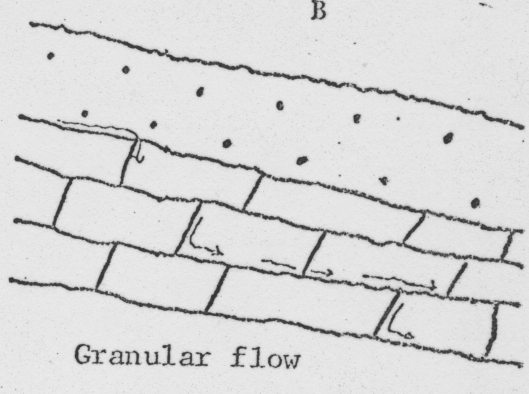
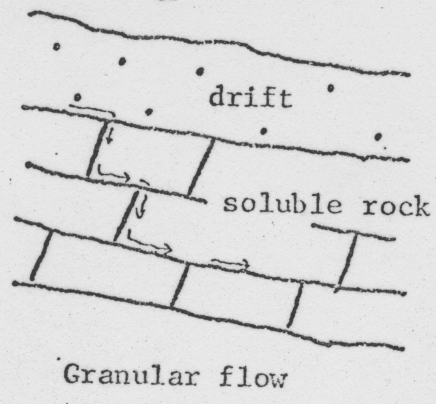
6 - Jubilee Fm., dolomite

drawn above that the subsurface flow in the Phantom Sink Creek area is not through gypsiferous materials, and from the assumption that large sinkholes are formed above gypsum beds. It seems that in order to make the first two factors above compatible with the third, sinkhole development occurs along the line of contact between strata 13 and 14.

There are two possible modes of sinkhole formation - continued preferred solution in a particular location, or sudden collapse of material at a point into a void. Both modes involve preferential solution of certain lines or points, as shown in Figure 17. Case b, however, requires the groundwater flow regime to be one of massive pipe development. In the Canal Flats instance there is little to suggest that this has taken place. Although there is some evidence for the existence of ordered flow paths in certain places (particularly the Phantom Sink and Tufa Creeks areas) there is reason to assume that these paths are only very poorly developed. Flow from sinkholes 9 and 10 to the associated risings is very slow (the flow time is greater than four days for a distance of  $\frac{1}{4}$  mile, over a vertical distance of 250'), and the risings are very small and poorly integrated. It is to be expected that minor pipe development should begin where certain conditions exist - where the drainage gradient is higher, or where there is a more plentiful supply of undersaturated water. These two conditions correspond to the observed distribution of sinkholes - in association with tributary valleys (producing a locally increased drainage gradient) and along the break in slope above and to the east of Coyote Creek (the series of sinkholes to the north of sinkholes 11, 10 and 9), and along

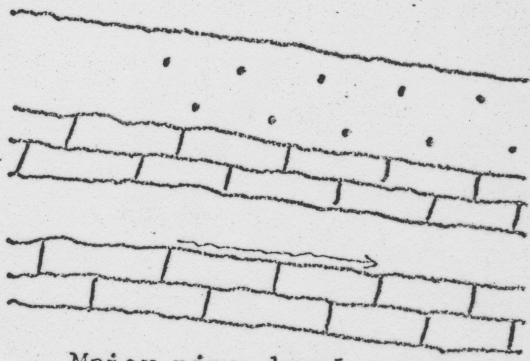
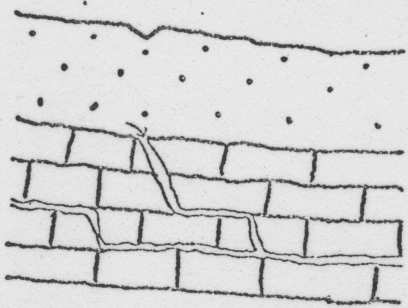
A

B



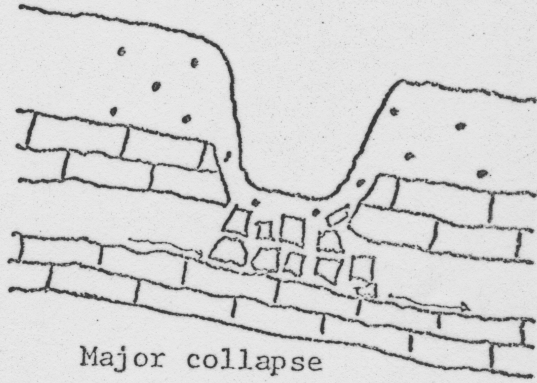
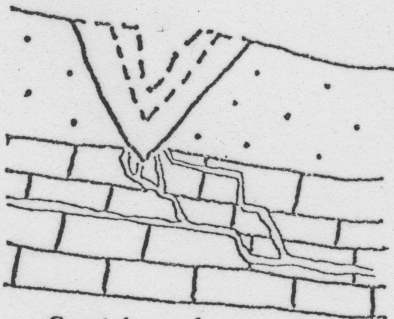
Granular flow

Granular flow



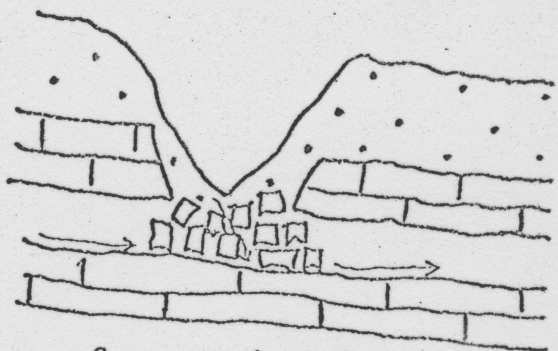
Some minor pipe development, with associated sapping of drift

Major pipe development



Continued sapping

Major collapse



Some sapping of drift

Figure 17. Modes of sinkhole development.

the limestone-gypsum contact (particularly sinkholes, 1, 2, 3, and 12 and 13). Many sinkholes are located in positions where these two effects might combine, depending on the exact position of the gypsum strata.

## CHAPTER FIVE

### DISCUSSION AND CONCLUSION

#### 1. Discussion of Saturation Measures

Thus far, no use has been made of the now classical Trombe graphs which have been adopted by numerous workers in karst studies (for example, Ford 1964). The curves now used to determine saturation on a plot of pH against  $\text{Ca}^{++}$  were developed by Picknett (1964) assuming that  $\text{HCO}_3$  can be regarded as a function of pH and  $\text{Ca}^{++}$ . Figures 18 through 21 illustrate the differences between the saturation values of all samples used in this thesis as described by SATCAL and Trombe curves. It can be seen that in no instance is there complete agreement. Use of the Trombe graph necessitates the visual interpretation of the effect of temperature since there is a family of curves representing saturation at different temperatures.

In addition it is extremely difficult to derive a quantitative measure of saturation from a Trombe graph, and it is such data which is necessary to determine any relationships between degree of saturation and other variables. Further consideration of the differences between the Picknett curves and those of  $\text{Ca}^{++}$  vs SATCAL suggest that they arise largely from the use of different values of  $K_s$ , the solubility constant of calcite. The work of Frear and Johnston (1929) and Harned and Scholes (1941) which Picknett used as sources for  $K_s$  and  $K_2$  have been reviewed

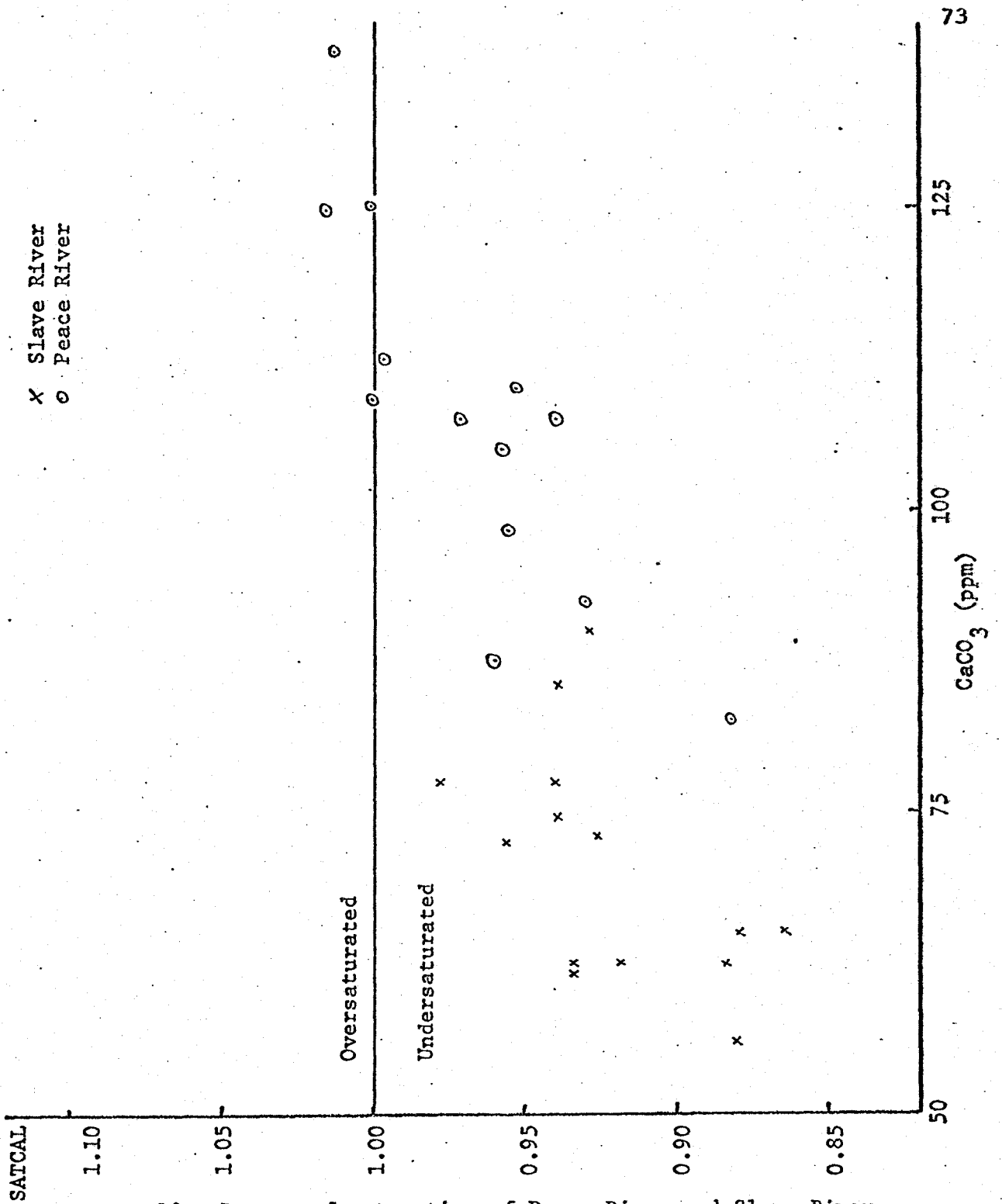


Figure 18. Degree of saturation of Peace River and Slave River in 1968.

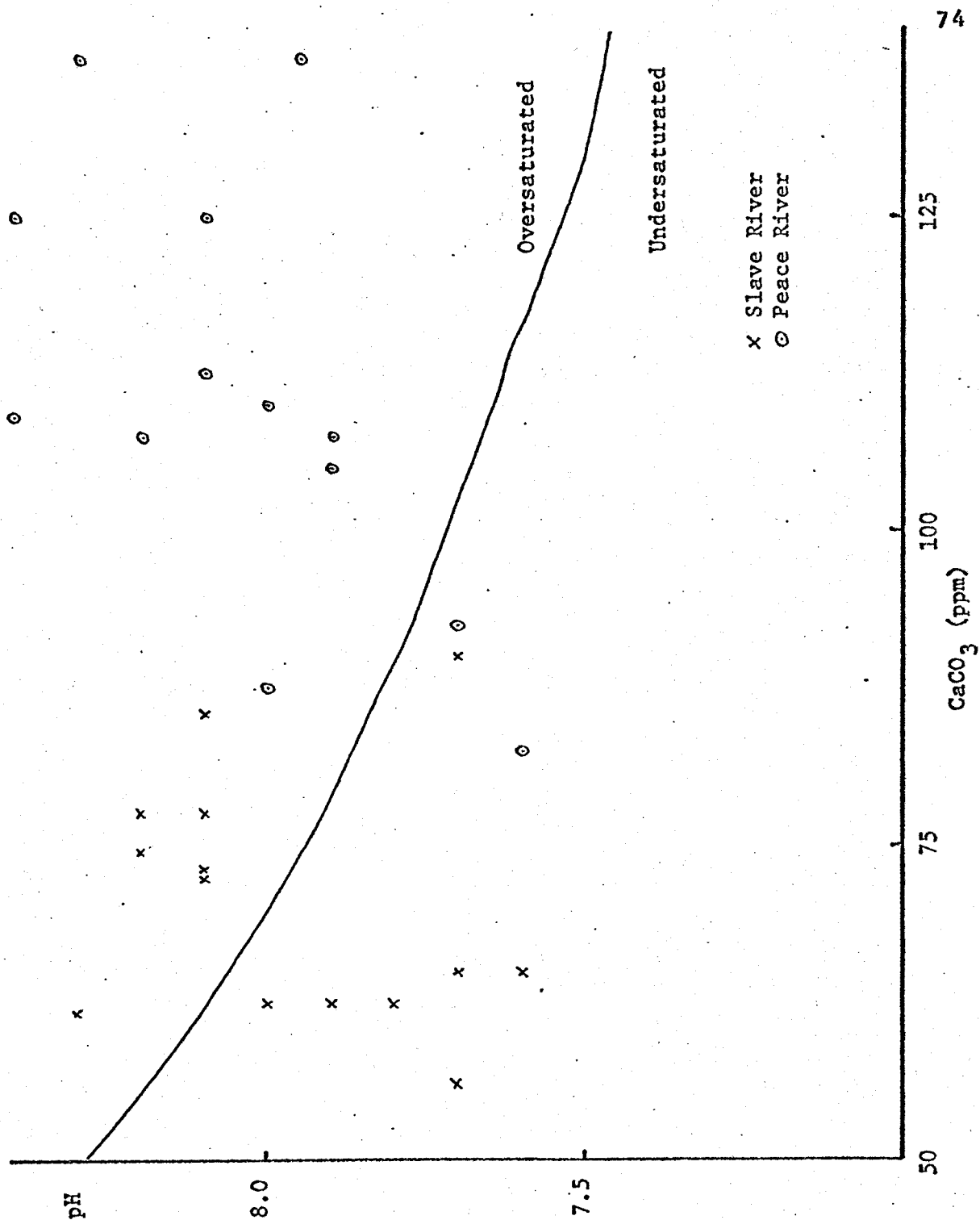


Figure 19. Trombe graph for Peace River and Slave River, 1968, using Picknett's curve.

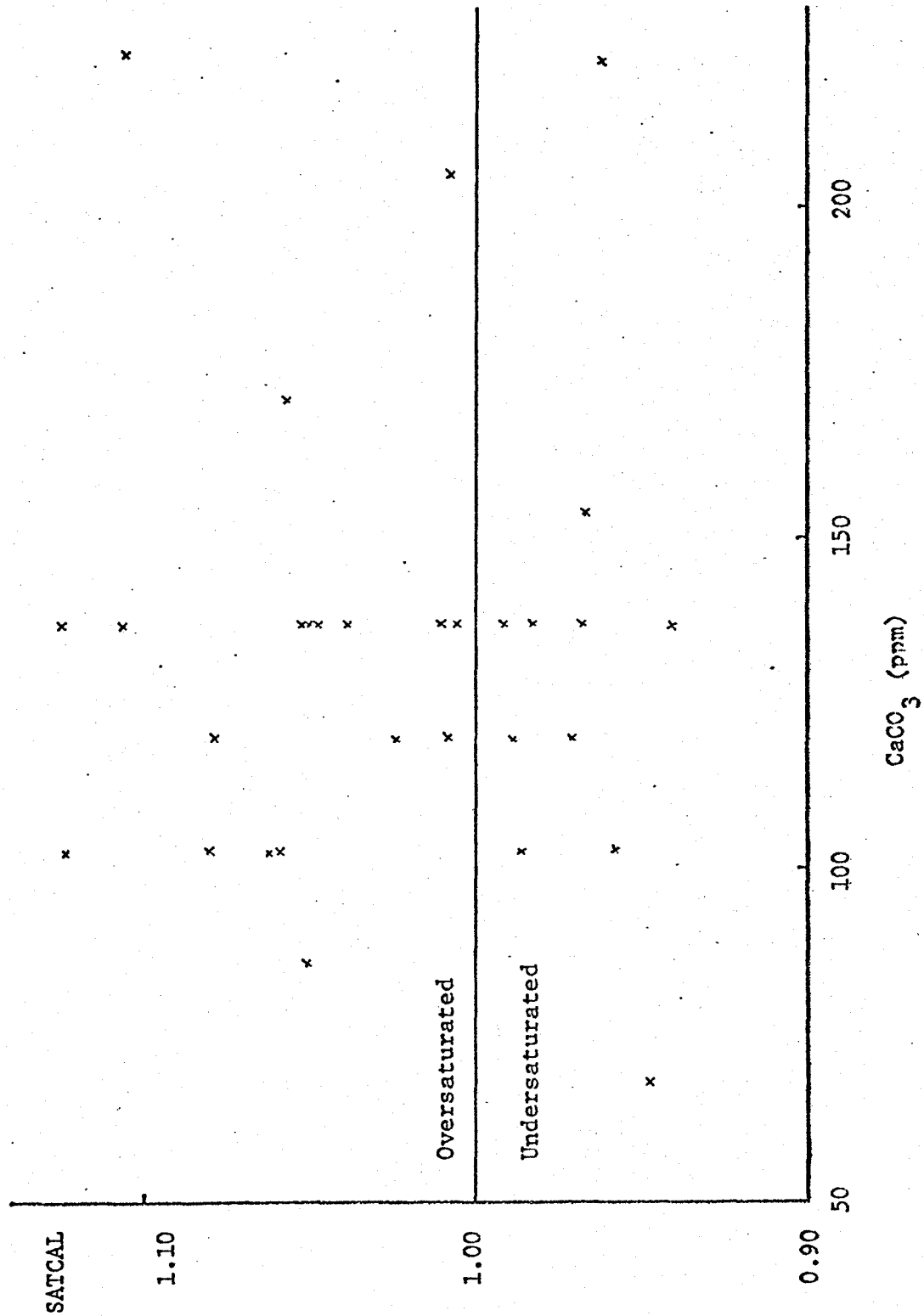


Figure 20. Degree of saturation for samples in the Canal Flats area, 1968.

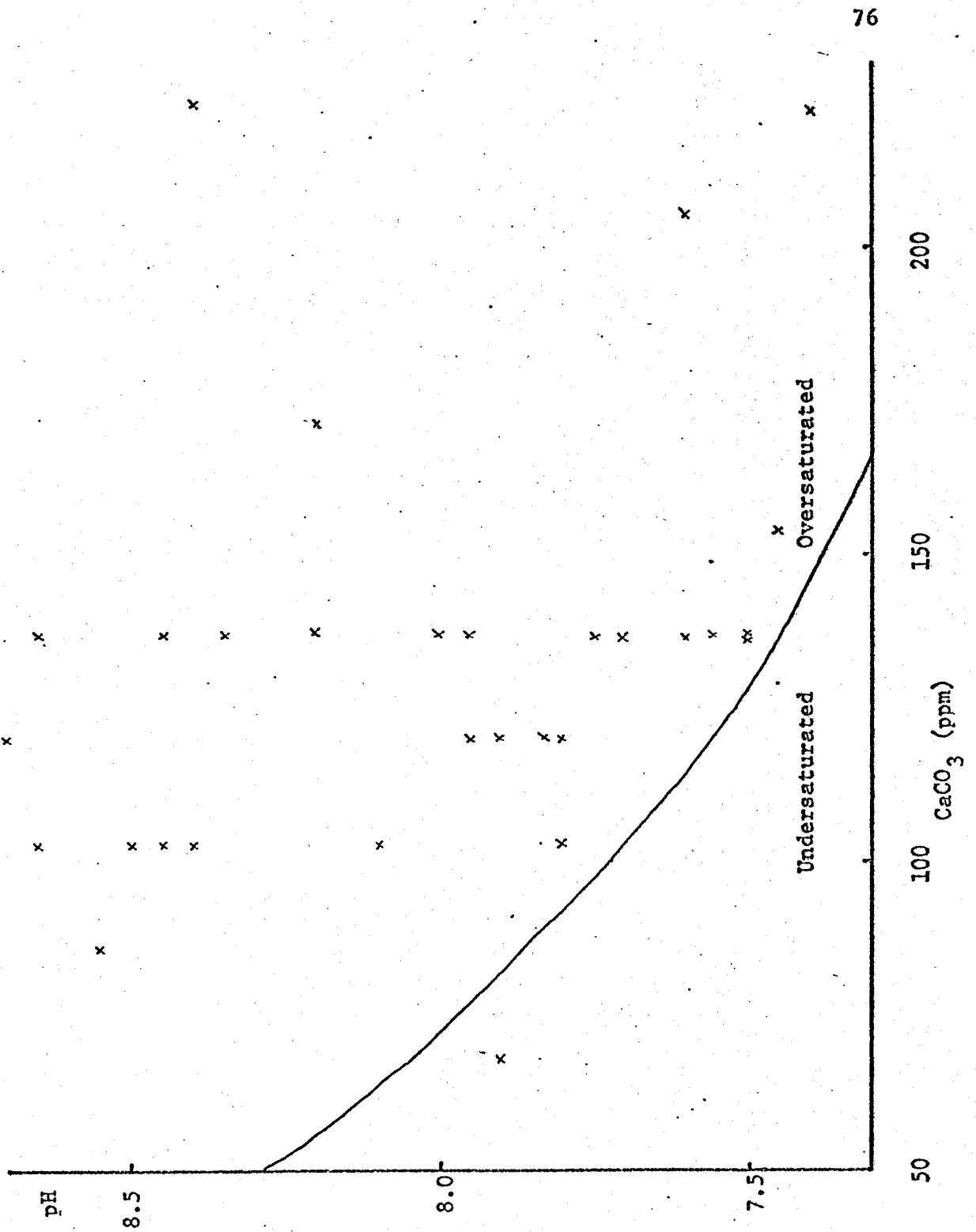


Figure 21. Trombe graph for samples in the Canal Flats area, 1968, using Picknett's curve.

by Larson and Buswell (1942). This latter paper presents a complete treatment of the topic of carbonate equilibria and has been used as a source by Garrels and Christ (1964). The value for  $K_s$  of  $7.08 \times 10^{-9}$  at  $10^\circ\text{C}$  is now commonly accepted, and it would seem that Picknett's calculated value of  $2.65 \times 10^{-9}$  is in error. A recalculation of the values of SATCAL using Picknett's constants compares well with the pH - Ca curve in predicting the degree of saturation (Figure 22). Many workers in karst geomorphology have remarked on the seemingly universal tendency for groundwater to be saturated, and yet to have a capacity to further erode limestone. Insofar as the index SATCAL used in this thesis estimates saturation to be lower for any given sample than does Picknett's method, and shows nearly all groundwater samples to be slightly undersaturated it would seem to be more in keeping with observed characteristics.

A review of other methods of estimating saturation commonly used in karst studies has been given by Stenner (1969). Most of these involve the measurement of the change of one variable, pH or  $\text{Ca}^{++}$ , of the sample when mixed with pure calcium carbonate or the determination of the excess  $\text{CO}_2$  of the sample. Stenner notes that the objections to all these methods are that they require that the sample should not change between collection and analysis, and that they involve bringing the sample to a state of exact saturation. This is generally accomplished by mixing with calcium carbonate but it seems that any agitation of the sample is likely to result in some loss of  $\text{CO}_2$ . The main advantage of the method used in this thesis is that it does not require samples to be stored. Both the

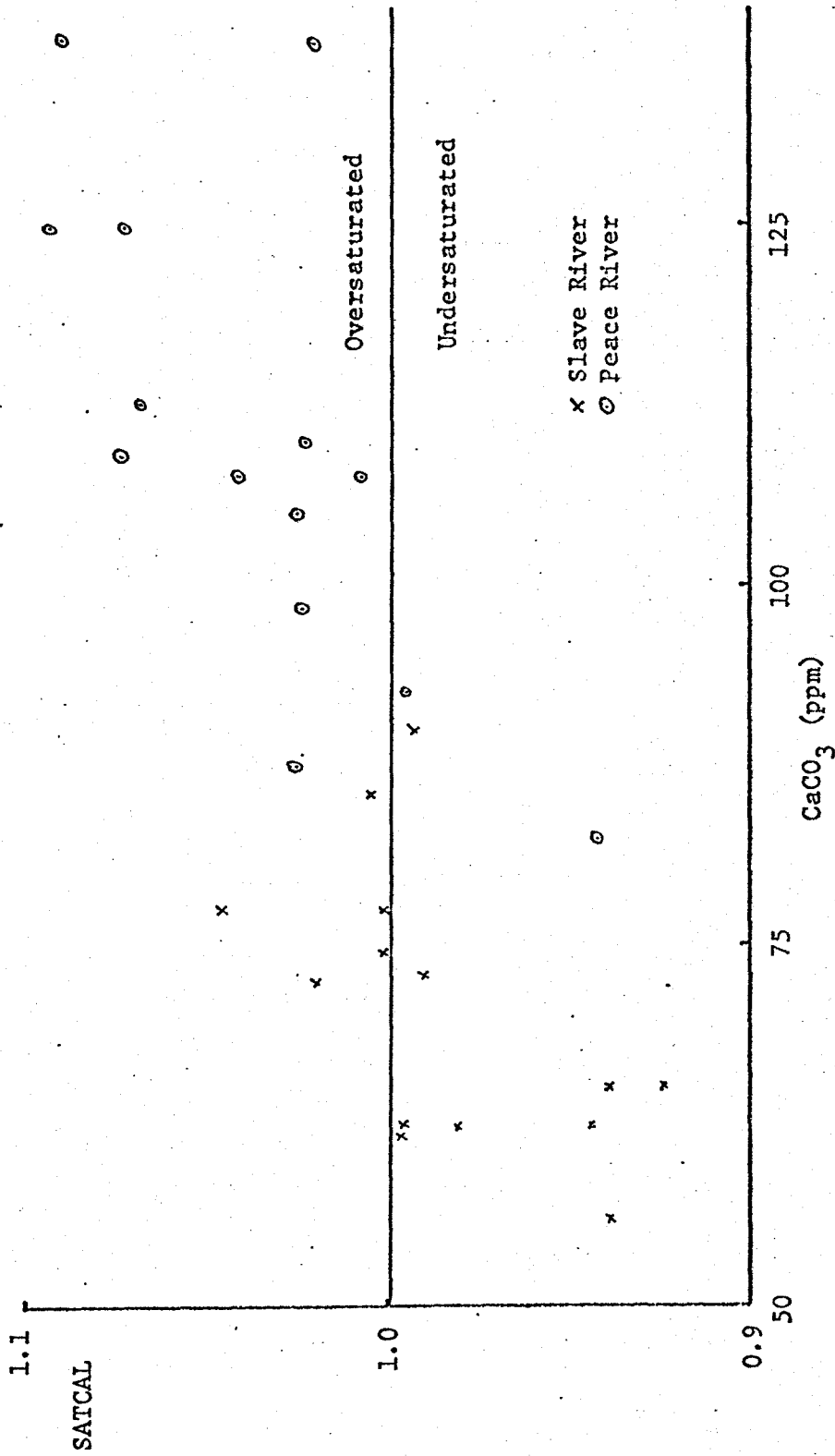


Figure 22. Degree of saturation of Peace River and Slave River, 1968, using Picknett's value for  $K_s$ .

$\text{Ca}^{++}$  and  $\text{Mg}^{++}$  and the  $\text{HCO}_3^-$  determinations are simple and can be performed in the field, thus ensuring that no deterioration due to storage or temperature changes can occur. In addition, if complete data is available from other sources, the degree of saturation can still be readily calculated and if such data, or field data, is complete for a wider range of elements and ions it is possible to use activity coefficients to give a more thermodynamically correct estimation. The importance of this even in areas of very low concentrations is shown in the case of the Peace and Slave Rivers where, with a  $\text{Ca}^{++}$  content of 20-40 ppm. the use of activities changes SATCAL values by 0.02, enough to change one sample from an oversaturated to an undersaturated state. In the case of Benchmark Creek, where  $\text{Na}^+$  and  $\text{Cl}^-$  ions are present in large quantities, the index SATGYP shows all samples to be saturated if activities are not considered; otherwise, all samples are considerably undersaturated.

## 2. Conclusions

It appears that chemical analysis of karst waters can lead to certain geomorphologically significant deductions. The simpler nature of the solution process in gypsum areas is illustrated by the analysis of the behaviour of Benchmark Creek. In this instance the index SATGYP shows a strong correlation with discharge, (Figure 11) with  $r = 0.83$  indicating the relationship to be significant at the 0.01 level. No other surface flow in the Wood Buffalo area considered in this thesis shows any such relationship, so it is pertinent to consider the distinguishing features of Benchmark Creek. It is the only stream to be fed mainly by an underground source, to have a high  $\text{Na}^{++}$  and  $\text{Cl}^-$  content,

and to originate mostly from gypsum. It is to be expected that a stream which is fed to a considerable extent by surface runoff will not demonstrate any relationship between groundwater chemistry and discharge unless the proportion of flow contributed from an underground flow network remains constant for all flows. It is also evident that if any relationship is to exist, the nature of the rock/water interface must be such that it does not represent an independent variable. For example, if a stream flows through an underground channel of varying cross sectional geometry the contact between rock and water is not solely a function of discharge (or, if the cross-section is constant, of velocity), but also of stage.

These considerations suggest that where a relationship is observed the greater part of the flow originates from similar sources (in the case of Benchmark Creek these are subterranean conduits) and the flow is such that the rock/water contact is a simple function of discharge. This may be taken to indicate phreatic flow in simple pipes, since any vadose situation is likely to lead to a stage/contact relationship as suggested above. The lack of a similar SATCAL/discharge relationship for Benchmark Creek may be due to a complicating factor confusing any pH/discharge relationship, or may reflect on the nature of the limestone (or dolomite) water interface: if this were entirely vadose, then a relationship would not be expected. Any combination of such effects would serve to further complicate the interactions.

In the Canal Flats area, much of which can be considered to be a limestone terrain, it has proved possible to determine the probable location and extent of the major gypsum deposits. Hydrochemical measure-

ments, in conjunction with a dye test on the east side of Coyote Creek, allow the construction of a model of the groundwater flow regime. A Hypothesis of sinkhole development and location can also be derived, which in turn allows these features to be considered as geologic indices in their own right.

Areal variations in chemical parameters can, like temporal variations, lead to conclusions of some geomorphic significance. With better data it would be possible to locate certain deposits (for example, gypsum) with no great outlay of labour, time or money. Taken individually no one parameter or index can be so used, but together SATCAL, SATGYP,  $\text{Ca}^{++} : \text{Mg}^{++}$  and  $\text{Ca}^{++} : \text{SO}_4^{=}$  yield significant information.

## APPENDIX A

### COMPUTER PROGRAMS

Two programs written in FORTRAN IV for use on a CDC 6400 computer are used in this thesis. One, SOLDATA, computes saturation indices for calcite and dolomite, the other, GYPINFO, the index for gypsum and the  $\text{Ca}^{++}/\text{SO}_4^{=}$  ratio. These were not amalgamated as SOLDATA alone is used for routine analysis of other carbonate data, but they are in all other respects identical.

One of the requirements of both programs is that they should be capable of processing data in a number of forms. There appear to be as many conventions for reporting analyses as there are analysts, but the systems used in this thesis are:

- a) Water survey of Canada analyses, reported in ppm of the respective ions
- b) Results obtained from the use of Hach water analysis kits, which give  $\text{Ca}^{++}$ ,  $\text{Mg}^{++}$  and alkalinity in terms of grains/U.S. gallon  $\text{CaCO}_3$ , and  $\text{Cl}^-$  in ppm NaCl
- c) Specific ion electrodes for  $\text{Ca}^{++}$  and  $\text{Cl}^-$  which give measures of the activity in terms of molar concentrations.
- d) EDTA titrations for  $\text{Ca}^{++}$  and  $\text{Mg}^{++}$ , and a potentiometric titration for alkalinity using HCl.

All of the above systems may report temperature in  $^{\circ}\text{C}$  or  $^{\circ}\text{F}$ .

Output from both programs can take one of two forms - printed or

plotted or a print-out graph. In the case of SOLDATA the graph option also produces a Trombe graph of the data points. A further option on both programs allows the activity coefficients to be used in all calculations. If this option is used together with the print option the total ionic strength is printed. These options are controlled by one data card: the system used for the derivation of the data input to the program is coded for each record, so that all data systems may be processed in a single run. The program listing for SOLDATA is given below: that for GYPINFO is essentially identical.

```

PROGRAM SOLDATA (INPUT,OUTPUT,TAPE6=OUTPUT)
C   FIRST DATA CARD IS OPTION TO USE ACTIVITIES (COL 1-4 NOT ZERO
C   AND PRINT OR PLOT O/P. (COLS 5-8 ZERO FOR PRINT)
C   SEPARTE BLOCS OF DATA HAVE SAME OPTION, AND ARE SEPARATED BY DL
C   CARD. LAST DATA CARD OF WHOLE JOB HAS SERIAL 9999999.
DIMENSION PK3 (5), PKDOL (5), PK2(5)
DIMENSION G(50), K(50), m(50)
DIMENSION E(6),F(6)
REAL MG,MGM
C   VALUES OF PK3, PK2 TAKEN FROM GARRELS AND CHRIST. VALUES FOR
C   PKDOL ADAPTED FROM GARRELS
DATA PK3/8.02,8.09,8.15,8.22,8.26/,PKDOL/15.8,15.94,16.22,16.30,
116.50/,PK2/10.62,10.96,10.49,10.45,10.30/,ACONC/0.0055/,VSAMP/2
2,A/0.5042/
DATA E/240.,200.,160.,120.,80.,40./,F/6.5,6.63,6.77,6.97,7.29,7.
1/
J=0
READ 400,OP,G
IF(G.NE.0.) GO TO 20
PRINT 100
20 READ 201,SERIAL,CA,MG,ACID,FI,PH,STPH,T,ALK,UNIT
IF(SERIAL.EQ.9999999..OR.SERIAL.EQ.0.) GO TO 84
J=J+1
C   CONVERT TEMP TO CENTIGRADE. IF IN FAHRENHEIT
IF (UNIT.GT.100..OR.UNIT.LT.0.) 1,2
1 T=((T-32.)*5.)/9.
2 IF (T.GE.25..OR.T.LT.0.) GO TO 50
C   CALCULATE ALKALINITY IF TITRATION USED OR PROCEED IF HIGH
C   ALKALINITY VALUES USED
22 IF (ACID.EQ.0..OR.ALK.GT.0.) 4,3
3 HFIT=10.**(-FI*PH)
ALKC=((ACONC*ACID)-(VSAMP*ACID)*HFIT)/VSAMP
IF (ALKC.LE.0.) 60,4
C   CONVERT CONCENTRATIONS TO MOLES PER LITRE
4 IF (UNIT.LT.50.) 5,6
5 CA=CA*17.1
MG=MG*17.1
6 IF(UNIT.EQ.99..OR.UNIT.EQ.102.) 17,16
17 CAM=(CA/40.)*10.**(-5.)
MGM=(MG/24.)*10.**(-5.)
GO TO 18
16 CAM=CA*10.**(-5)
MGM=MG*10.**(-5.)
18 IF (UNIT.EQ.99..OR.UNIT.EQ.102.) 92,90
90 IF (ACID.EQ.0..AND.ALK.GT.0.) 7,8
7 ALK=ALK*(17.1/61.)*10.**(-3)
GO TO 91
92 ALK = (ALK/61.)*10.**(-3)
91 ALK =ALK
C   CALCULATE P VALUES FOR CA AND ALKALINITY
8 IF(OP.EQ.0.) 13,81
81 SSI=(0.5*((CAM*4.)+(MGM*4.))+ALKC)
SI=SSI**(0.5)
PCA=(ALOG10(CAM)-(((SI*4.)/(1.+SI))-0.2*SSI))*(-1.)
PALKC=(ALOG10(ALKC)-(((SI*4.)/(1.+SI))-0.2*SSI))*(-1.)
GO TO 80
13 PALKC=ALOG10(ALKC)*(-1.)
PCA=ALOG10(CAM)*(-1.)
C   CALCULATE SOLUBILITY CONSTANT FOR CALCITE
20 I=(1/5.)+1.
APK2=PK2(I)

```

```

APKS=PKS(I)
APKDOL=PKDOL(I)
PKSC=PCA+PALKC+APK2-STPH
C CALCULATE INDEX OF SATURATION FOR CALCITE
SATCAL=APKS/PKSC
X=CA
Y=SATCAL
N=(SERIAL/10000.)+1.
IF(G.EQ.0.) 82,83
82 IF(MG.EQ.0.) 9,10
9 SATDOL=0.
GO TO 11
10 PMG=ALOG10(MGM)*(-1.)
C CALCULATE SOLUBILITY CONSTANT OF DOLOMITE
PKDOLC=PCA+PMG+2.*PALKC+2.*APK2-2.*STPH
C CALCULATE INDEX OF SATURATION FOR DOLOMITE
SATDOL=APKDOL/PKDOLC
11 PRINT 101,SERIAL,CA,MG,ALKC,T,STPH,SATCAL,SATDOL,CA,MGM
30 GO TO 20
50 PRINT 300,SERIAL
J=J-1
GO TO 20
60 PRINT 301,SERIAL
J=J-1
GO TO 20
83 CALL PLOTPT(X,Y,N)
C HOPEFULLY NOW PLOT TRIMBE CURVE
Q(J)=STPH
R(J)=CA
M(J)=(SERIAL/10000.)+1
GO TO 20
84 IF(G.EQ.0.) 70,85
85 CALL SCALE (60.,320.,0.85,1.2)
CALL OUTPLT
I=J
J=0
DO 45 K=1,I
J=J+1
CALL PLOTPT (Q(J),R(J),M(J))
45 CONTINUE
DO 46 L=1,6
CALL PLOTPT(F(L),E(L),10)
46 CONTINUE
CALL SCALE (6.6,8.6,50.,320.)
CALL OUTPLT
IF(SERIAL.EQ.9999999.) 40,20
70 PRINT 302
IF(OP.EQ.0.) 48,49
48 PRINT 998
GO TO 40
49 PRINT 999
40 STOP
100 FORMAT(*1 SERIAL CA MG ALKC
IT STPH SATCAL SATDOL CA MG ALKC
101 FORMAT (1H0,F12.0,2F12.4,F12.0,4F12.4,2F12.8)
201 FORMAT (F8.0,2F6.2,3F6.3)
300 FORMAT (1X,F8.4,*TEMP GREATER THAN 25 DEG C OR LESS THAN ZERO*)
301 FORMAT (1X,F8.4,*ERROR IN ALKALINITY TITRATION: CALCULATED VALUE

```

1IN DEG C. IN SATCAL, SATDOL SATURATION = 1.0\*/IX,\*IF SATDOL = 0.0  
2NO CALCULATION AS MG = 0.. CAN; MG IN MOLES PER LITER \*)  
400 FORMAT(2F4.2)  
998 FORMAT(IX,\*ACTIVITIES NOT USED\*)  
999 FORMAT (IX,\*ACTIVITIES USED\*)  
END

CD TOT 0127

## APPENDIX B

### ALKALINITY DETERMINATION

The method of determining  $\text{HCO}_3^-$  used in this thesis is based on that described by Rainwater and Thatcher (1960). It is a potentiometric titration with HCl to an end-point of between pH3 and pH4. The accurate end-point (measured by a Metrohm pH meter) is subsequently incorporated into the calculation. The use of this technique results in increased accuracy since, if the  $\text{HCO}_3^-$  concentration of the sample is small, the end-point is reached quickly and the problems of attaining a fixed end-point are severe.

The titration will estimate all carbonate species present (which represents 'total alkalinity'), but within the range of pH encountered in the samples used in this thesis (7.5 to 9.0) well over 90% of this sum is  $\text{HCO}_3^-$  (see Figure 23).

$\text{HCO}_3^-$  is then calculated as:

$$\text{HCO}_3^-(\text{eq/l}) = \frac{H_a V_a - H_f (V_a + V_s)}{V_3}$$

where =  $(\text{H}^+$  of HCl used (here 0.003N)  
= volume of acid added in titration (ml)  
= final  $(\text{H}^+)$  of titration  
= volume of sample used (here 25ml).

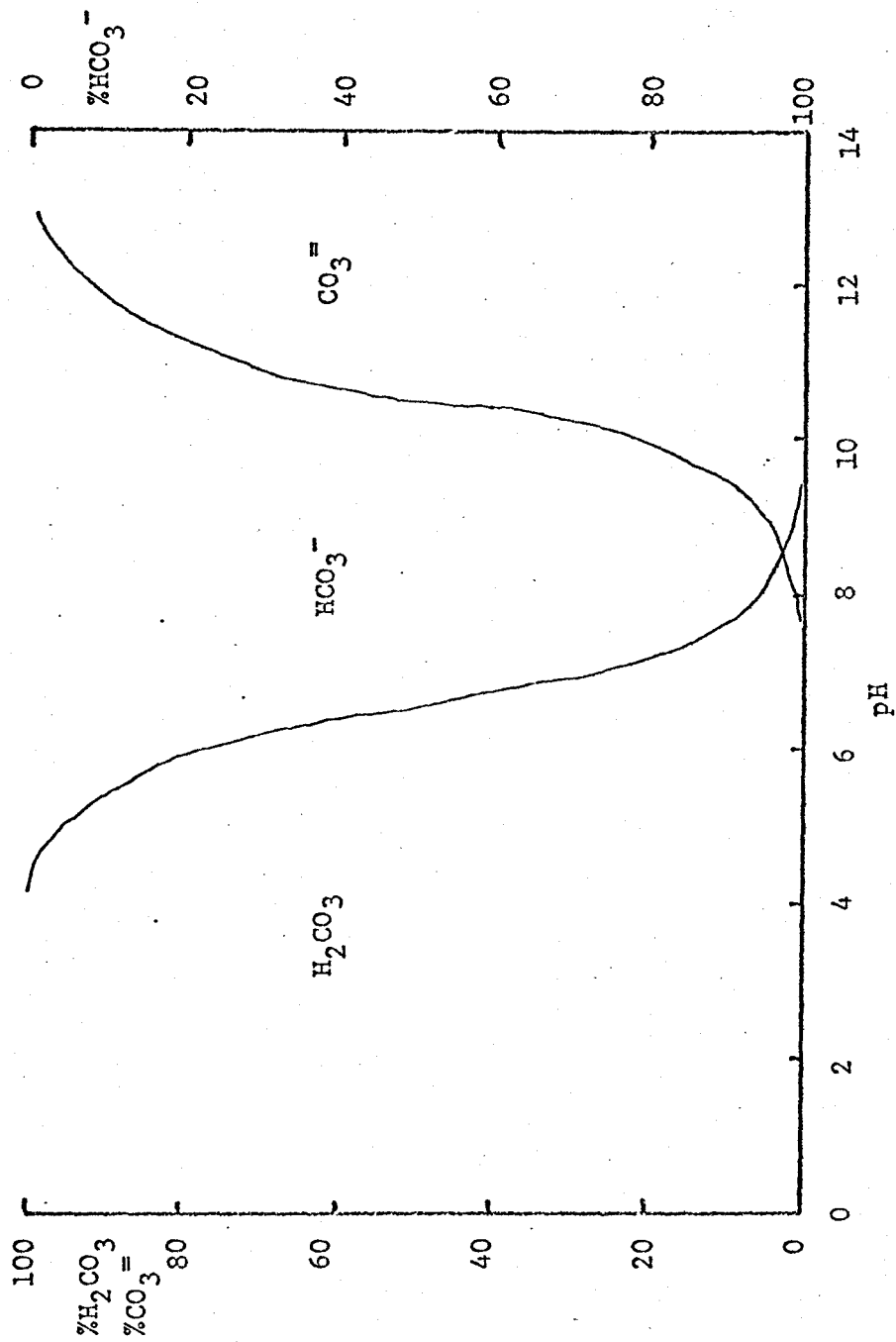


Figure 23. Distribution of carbonate species for all values of pH.

## BIBLIOGRAPHY

- Ashton, K., "The Analysis of Flow Data from Karst Drainage Systems," Trans. Cave Research Group of Great Britain 7 (2), pp 161-203.
- Atkinson, T, and Drew, D. P., 1967, "Mendip Karst Hydrology Research Project, Phases I and II," Wessex Cave Club Occasional Pub. Series 2, Number 1.
- Back, W. and Hanshaw, B. B., 1965, "Chemical Geohydrology," Chapter II in "Advances in Hydroscience 2," ed. Van Te Chow, Academic Press.
- Back, W, Cherry, R. N., and Hanshaw, B. B., 1966, "Chemical Equilibrium Between the Water and Minerals of a Carbonate Aquifer," (3), pp 119-126, Bull. Nat. Speleol. Soc. Amer. 28 (3)
- Brandon, L. V., 1965, "Groundwater Hydrology and Water Supply in the District of Mackenzie, Yukon Territory and adjoining parts of British Columbia," Geol. Surv. Can. Paper 64-39.
- Brown, M. C., Wigley, T. L., and Ford, D. C., "Water Budget Studies in Karst Aquifers," Jour. Hydrol. 9 (1), pp 113-116.
- Camsell, C., 1917, "Salt and Gypsum Deposits of the Region between Peace and Slave Rivers, Northern Alberta," Geol. Surv. Can. Sum. Rpt. 1917, pp 134-145.
- Davies, 1962, "Ion Association", Butterworth.
- Douglas, I., 1968, "Field Methods of Water Hardness Determination," British Geomorphological Research Group, Tech. Bull. 1.
- van Everdingen, O, 1969, "Degree of Saturation with Respect to  $\text{CaCO}_3$ ,  $\text{CaMg}(\text{CO}_3)_2$  and  $\text{CaSO}_4$  for some Thermal and Mineral Springs in the S. Rocky Mountains, Alberta and B.C.," Can. Jour. Earth Sci. 6 (6), pp 1421-1431.
- Ford, D. C., 1964, "Calcium Carbonate Solution in Central Mendip Caves," Proc. Univ. Bristol Speleol. Soc. 11 (1), pp 46-53.
- Frear, G. L. and Johnston, J, 1929, "The Solubility of Calcium Carbonate (calcite) in Certain Aqueous Solutions at  $25^\circ$ ," Jour. Amer. Chem. Soc. 51, p 2082.

- Garrels, R. M. and Christ, C. L., 1965, "Solutions, Minerals and Equilibria," Harper and Row.
- Jakucs, L., 1959, "Neue Methoden der Höhlenforschung in Ungarn," Die Höhle 4.
- Kramer, J. R., 1969, "Thermodynamic Summary of Minerals, Gases and Ions as a Function of Temperature," Tech. Memo 69-2, Dept. of Geology, McMaster University.
- Larson and Buswell, 1942, "Calcium Carbonate Saturation Index and Alkalinity Interpretation," Journ. Amer. Water Works Assn. 34 (11), pp 1667-1682.
- Leech, G. B., 1954, "Canal Flats, B.C.," Geol. Surv. Can. paper 54-7.
- Lesick, H. S., Chief Chemist, Water Quality Division, Inland Waters Branch, Department of Energy, Mines and Resources, Calgary, Alta.
- Metler, A. V. and Ostroff, A. G., 1967, "The Proximate Calculation of Gypsum in Natural Brines from 28° to 70°C," Environ. Sci. and Technol. 1 (10), p 815.
- Novakowski, N., Staff Mamalogist, National and Historic Parks Branch, Department of Energy, Mines and Resources, Ottawa.
- Picknett, R. G., 1964, "A Study of Calcite Solutions at 10°C," Trans. Cave Research Group of G.B. Volume 7 (1), pp 39-62.
- Pinder, G. F. and Jones, J. F., 1969, "Determination of the Groundwater Component of Peak Discharge from the Chemistry of Total Runoff," Water Resources Research 5 (2), p 438.
- Pitty, A. F., 1966, An Approach to the Study of Karst Water, Univ. Hull Occ. Papers in Geog. 5, 1966, pp 70.
- Pitty, A. F., 1968, Some features of Calcium Hardness fluctuations in two Karst Streams and their possible value in geohydrological studies, Journ. Hydrol. 6, p 202-208.
- Rainwater, F. H. and Thatcher, L. L., 1960, "Methods for Collection and Analysis of Water Samples," V.S. Geol. Surv. Water Supply Paper 1454 301 p.
- Soper, J. D., 1941, "History, Range and Home life of the Northern Bison," Ecol. Monog. II, pp 347-412.
- Smith, D. I. and Mead D. G., 1962, "The Solution of Limestone," Proc. Univ. Bristol Speleol. Soc. 9 (3), pp 188-211.
- Steane, R. D., 1969, "The Measurement of the Aggressiveness of Water towards Calcium Carbonate," Trans, Cave Research Group of G.B. 11 (3), pp 175-200.
- Zverev, V. P., 1965, "Sulfate-Calcium Equilibrium in Subsurface Waters," Doklady Akad. Nauk S.S.R. 164, pp 118-120.